

## Variational calculation of the ground state of $^{16}\text{O}$

Steven C. Pieper and R. B. Wiringa

*Physics Division, Argonne National Laboratory, Argonne, Illinois 60439*

V. R. Pandharipande

*Department of Physics, University of Illinois, Urbana, Illinois 61801*

(Received 18 June 1992)

We report variational calculations of the ground state of  $^{16}\text{O}$  with realistic two- and three-nucleon interactions. The trial wave function is constructed from pair- and triplet-correlation operators acting on a product of single-particle determinants. These operators include central, spin, isospin, tensor, spin-orbit, and three-nucleon potential components. Expectation values are evaluated with a cluster expansion for the noncentral correlations; terms in the expansion are evaluated exactly using Monte Carlo integration. The optimal trial function is obtained by minimizing the energy through the four-body cluster level. Results are reported for the ground-state binding energy, nucleon density and momentum distributions, charge form factor, and longitudinal structure function. They are also compared with the available results for few-body nuclei and nuclear matter with the same interactions.

PACS number(s): 21.60.-n, 21.10.-k, 25.30.-c, 27.20.+n

### I. INTRODUCTION

A major problem in nuclear physics is to understand how nuclear structure comes about from the underlying interactions between nucleons. Elastic nucleon-nucleon scattering data can be accurately described with a variety of "realistic" two-body potentials. All these realistic potentials have large spin, isospin, and tensor terms. In addition, three-nucleon potentials are significant on the scale of the binding energy. Consequently, many-body calculations of nuclear ground states are extremely challenging, and many fundamental issues, including the stability of light nuclei against breakup and the origin of the spin-orbit splitting in the shell model, have not been addressed satisfactorily to date.

We want to solve the many-body Schrödinger equation  $H\Psi = E\Psi$  for arbitrary size nuclear systems, where

$$H = \sum_i \frac{-\hbar^2}{2m} \nabla_i^2 + \sum_{i<j} v_{ij} + \sum_{i<j<k} V_{ijk} \quad (1.1)$$

$$\equiv T + v + V, \quad (1.2)$$

and  $v_{ij}$  and  $V_{ijk}$  are two- and three-nucleon potentials that fit scattering data and few-body ground-state properties. Exact solutions, obtained by Faddeev [1] and Green's-function Monte Carlo (GFMC) [2] methods, are available only for  $A \leq 5$  nuclei at present. These calculations show that realistic  $v_{ij}$  give only  $\sim 85\%$  of the experimental binding energy and attribute the rest to  $V_{ijk}$ . Variational Monte Carlo (VMC) calculations [3] of the few-body binding energies are accurate within 4%. The infinite-body nuclear matter problem has been approximately solved with two-nucleon potentials by Brueckner-Bethe [4] methods and with two- and three-nucleon potentials by variational [5] methods, but the accuracy of these calculations is not firmly established, and the agreement with empirical data is only at the 10% level.

The first detailed calculations of larger nuclei with realistic interactions were made by Kümmel, Lührmann, and Zabolitzky [6], who studied  $^4\text{He}$ ,  $^{16}\text{O}$ , and  $^{40}\text{Ca}$  using the coupled-cluster method. Their most sophisticated calculation, designated Faddeev-Brueckner-Hartree-Fock-4, retained all two- and three-body and some four-body cluster contributions. In this approximation they obtained ground-state energies for the Reid [7] potential of  $-6.0$ ,  $-5.0$ , and  $-6.0$  MeV/nucleon, respectively, for  $^4\text{He}$ ,  $^{16}\text{O}$ , and  $^{40}\text{Ca}$ . The experimental values are  $-7.1$ ,  $-8.0$ , and  $-8.6$  MeV/nucleon. Their value for  $^4\text{He}$  is in good agreement with a variational result of  $-5.9$  MeV/nucleon and an exact GFMC result of  $-6.1$  MeV/nucleon. However,  $^{16}\text{O}$  is not stable with respect to breakup into four  $^4\text{He}$  nuclei with this interaction, while  $^{40}\text{Ca}$  is barely stable. They also made some calculations with an early version of the Tucson-Melbourne [8] three-nucleon potential, which lowered the binding energies to  $-8.2$ ,  $-7.2$ , and  $-8.1$  MeV/nucleon, leaving  $^{16}\text{O}$  still unstable by 1 MeV/nucleon. Further, their  $V_{ijk}$  was averaged over the third particle to make an effective density-dependent two-nucleon potential, and this has since been shown to be a poor approximation [9].

The first VMC calculation of  $^{16}\text{O}$  was made by Carlson and Kalos [10], but they used a semirealistic version of the Reid potential without  $V_{ijk}$  and had large sampling errors. More recently, we reported initial results for a variational method using a cluster expansion with Monte Carlo integration (CMC) for evaluating expectation values [11]. These studies have been made for a realistic Hamiltonian containing the Argonne  $v_{14}$  two-nucleon [12] and Urbana VII three-nucleon [13] potentials. The present paper is an updated and more complete report of these studies.

The interactions and the variational wave function are described in Sec. II; the cluster expansions and the Monte Carlo methods are presented in Secs. III and IV, respec-

tively. We have used three different cluster expansions, and their results are compared in Sec. V. Sections VI and VII give the results obtained for  $^{16}\text{O}$  and compare them with those for the few-body nuclei and nuclear matter. The one- and two-body densities, charge form factor, momentum distribution, and longitudinal structure function, calculated from the optimum wave function, are reported in Sec. VIII, and we conclude with Sec. IX.

$$O_{ij}^{p=1,14} = 1, \tau_i \cdot \tau_j, \sigma_i \cdot \sigma_j, (\sigma_i \cdot \sigma_j)(\tau_i \cdot \tau_j), S_{ij}, S_{ij}(\tau_i \cdot \tau_j), \mathbf{L} \cdot \mathbf{S}, \mathbf{L} \cdot \mathbf{S}(\tau_i \cdot \tau_j), L^2, L^2(\tau_i \cdot \tau_j), L^2(\sigma_i \cdot \sigma_j), L^2(\sigma_i \cdot \sigma_j)(\tau_i \cdot \tau_j), (\mathbf{L} \cdot \mathbf{S})^2, (\mathbf{L} \cdot \mathbf{S})^2(\tau_i \cdot \tau_j). \quad (2.2)$$

(For convenience, we sometimes refer to these operators by the abbreviations  $c, \tau, \sigma, \sigma\tau, t, t\tau, b, b\tau, q, q\tau, q\sigma\tau, bb$ , and  $bb\tau$ .) Other potential models, such as the Paris [14] and Nijmegen [15] models, can be written in a similar form, but use  $\nabla^2$  operators instead of, or in addition to, the  $L^2$  operators. The long-range part of Argonne  $v_{14}$  is given by the usual one-pion exchange

$$v_{ij}^\pi = \frac{f_{\pi NN}^2}{4\pi} \frac{m_\pi}{3} X_{ij}(\tau_i \cdot \tau_j), \quad (2.3)$$

$$X_{ij} = Y_\pi(r_{ij})\sigma_i \cdot \sigma_j + T_\pi(r_{ij})S_{ij}, \quad (2.4)$$

where  $Y_\pi(r)$  and  $T_\pi(r)$  are the Yukawa and tensor Yukawa functions with a cutoff.

The Urbana VII three-nucleon potential [13] is a sum of long-range two-pion-exchange and short-range repulsive parts:

$$V_{ijk} = V_{ijk}^{2\pi} + V_{ijk}^R, \quad (2.5)$$

$$V_{ijk}^{2\pi} = A \sum_{\text{cyc}} (\{X_{ij}, X_{ik}\} \{\tau_i \cdot \tau_j, \tau_i \cdot \tau_k\} + \frac{1}{4} [X_{ij}, X_{ik}] [\tau_i \cdot \tau_j, \tau_i \cdot \tau_k]), \quad (2.6)$$

$$V_{ijk}^R = U \sum_{\text{cyc}} T_\pi^2(r_{ij}) T_\pi^2(r_{ik}). \quad (2.7)$$

The  $X_{ij}$  and  $T_\pi(r)$  are the same as in Argonne  $v_{14}$ , and the constants  $A$  and  $U$  were adjusted to give a good overall fit to the binding energies of few-body nuclei and nuclear matter in earlier variational calculations. The protons also interact with each other with a Coulomb potential calculated with a dipole proton charge form factor.

One feature of Argonne  $v_{14}$  is that the expectation value of the first six operators in  $v_{ij}$  is much larger than that of the remaining part. Including Urbana VII, the ordering of the expectation values in nuclear ground states is given by

$$\left| \left\langle \sum_{p=1,6} v_p(r_{ij}) O_{ij}^p \right\rangle \right| > \langle H \rangle > \left| \langle V_{ijk} \rangle \right| > \left| \left\langle \sum_{p=7,14} v_p(r_{ij}) O_{ij}^p \right\rangle \right|. \quad (2.8)$$

In  $^4\text{He}$ , for example, a variational calculation with this

## II. INTERACTIONS AND TRIAL FUNCTIONS

The Argonne  $v_{14}$  nucleon-nucleon potential [12] is written as a sum of operator terms:

$$v_{ij} = \sum_{p=1,14} v_p(r_{ij}) O_{ij}^p, \quad (2.1)$$

where

Hamiltonian gives  $-136, -30.5, -8.9$ , and  $+0.14$  MeV, respectively, for the above expectation values. This is not true for all interactions; e.g., in  $^4\text{He}$  with Nijmegen  $v_{ij}$ , the last term in Eq. (2.8) has an expectation value of  $-14$  MeV. The Nijmegen and Paris  $v_{ij}$  have operators  $O_{ij}^{p=9,12}$  with  $\nabla^2$  instead of the  $L^2$  in Eq. (2.2). Hence the  $O_{ij}^{p=9,12}$  terms in these models give large contributions via the dominant  $l=0$  partial waves, whereas in Argonne  $v_{ij}$  the  $O_{ij}^{p=9,12}$  are zero in  $l=0$  waves.

We assume that a good variational wave function for the ground state of a closed-shell nucleus can be expressed in the form of a product of two- and three-body correlation operators acting on a Jastrow wave function:

$$|\Psi_v\rangle = \left[ \prod_{i\neq j} (1 + U_{ijk}) \right] \left[ \mathcal{S} \prod_{i<j} (1 + U_{ij}) \right] |\Psi_J\rangle, \quad (2.9)$$

$$|\Psi_J\rangle = \left[ \prod_{i<j} f_c(r_{ij}) \right] \mathcal{A} |\Phi\rangle. \quad (2.10)$$

Here  $U_{ijk}$  and  $U_{ij}$  are operators containing the spin and isospin of particles  $ijk$  and  $ij$ , respectively,  $\mathcal{S}$  and  $\mathcal{A}$  are symmetrization and antisymmetrization operators,  $f_c(r_{ij})$  is a central pair-correlation function, and  $\Phi$  is an independent-particle wave function.

The ground-state wave function should be translationally invariant. The two- and three-body correlations are functions of the interparticle distances and, hence, satisfy this condition. By writing the one-body orbitals in  $\Phi$  as functions of

$$\tilde{\mathbf{r}}_i = \mathbf{r}_i - \mathbf{R}_{\text{c.m.}}, \quad (2.11)$$

$$\mathbf{R}_{\text{c.m.}} = \frac{1}{A} \sum_i \mathbf{r}_i, \quad (2.12)$$

we make the  $\Phi$  translationally invariant.

For  $^{16}\text{O}$  and  $^{40}\text{Ca}$ ,  $\Phi$  is conveniently expressed as a product of four determinants  $D_{\sigma\tau}$ , one each for spin up and down, neutrons and protons:

$$|\Phi\rangle = D_{\uparrow p} D_{\downarrow p} D_{\uparrow n} D_{\downarrow n}. \quad (2.13)$$

Each determinant contains  $A/4$  nucleons, and we can assume that  $D_{\uparrow p}$  contains nucleons 1 to  $A/4$ ,  $D_{\downarrow p}$  has nucleons  $A/4+1$  to  $A/2$ , etc. Then  $\mathcal{A}|\Phi\rangle$  in Eq. (2.10) is a sum over all partitions of the  $A$  nucleons into four groups of  $A/4$  nucleons, the sign of each term being such that  $\mathcal{A}|\Phi\rangle$  is antisymmetric.

In  $^{16}\text{O}$  each determinant could be constructed from one  $1s$  ( $\phi_{00}$ ) and three  $1p$  ( $\phi_{1m}$ ) wave functions, where

$$\phi_{1m}(\mathbf{r}) = X_l(r)Y_{lm}(\hat{\mathbf{r}}). \quad (2.14)$$

However, any set of orthogonal linear combinations of these functions will give the same determinant. In Monte Carlo calculations, it is more convenient to use the real functions

$$p_x(\hat{\mathbf{r}}) = x/r, \quad (2.15)$$

$$p_y(\hat{\mathbf{r}}) = y/r, \quad (2.16)$$

$$p_z(\hat{\mathbf{r}}) = z/r, \quad (2.17)$$

instead of the complex  $Y_{lm}$ 's.

In the present work, the radial wave functions  $X_l(r)$  are obtained from the bound-state solutions of a nucleon of mass  $m$  bound to a nucleus of mass  $(A-1)m$  by a Woods-Saxon wine-bottle potential

$$V(r) = V_s \left\{ \frac{1}{1 + \exp[(r - R_s)/a_s]} - \alpha_s \exp[-(r/\rho_s)^2] \right\}. \quad (2.18)$$

The parameters  $V_s$ ,  $R_s$ ,  $a_s$ ,  $\alpha_s$ , and  $\rho_s$  of  $V(r)$  are determined variationally.

Each operator in  $v_{ij}$  can induce a corresponding correlation. However, since the dominant features in the nucleon-nucleon phase shifts can be reproduced with a  $v_{ij}$  containing only the  $p=1-8$  terms, a reasonable choice for the pair correlation operator  $U_{ij}$  is

$$U_{ij} = \sum_{p=2,8} \beta_p u_p(r_{ij}) O_{ij}^p. \quad (2.19)$$

The eight pair-correlation functions  $f_c(r)$  and  $u_p(r)$  ( $p=2-8$ ) are obtained by solving a set of Euler-Lagrange equations [16] which minimize the two-body cluster contribution of a quenched potential:

$$\bar{v}_{ij} = \sum_{p=1,14} \alpha_p v_p(r_{ij}) O_{ij}^p, \quad (2.20)$$

to the energy of infinite nuclear matter at Fermi momentum  $k_F$ , with the boundary conditions

$$f_c(r > d) = 1, \quad (2.21)$$

$$u_p(r > d) = 0, \quad (2.22)$$

for  $p = \tau, \sigma, \sigma\tau, b$ , and  $b\tau$ ,

$$u_p(r > d_t) = 0, \quad (2.23)$$

for  $p = t$  and  $t\tau$ . The functions  $f_c(r)$  and  $u_p(r)$  are required to obtain their asymptotic values, at  $d$  or  $d_t$ , smoothly with zero first derivatives. The  $\alpha_p = 1$  for  $p = c, q, bb$ , and  $bb\tau$ , and  $\alpha_p = \alpha$  for all other  $p$ . Thus the variational parameters in the pair-correlation functions are the healing distances  $d$  and  $d_t$ , the Fermi momentum of nuclear matter  $k_F$  used in the Euler-Lagrange equations, the parameter  $\alpha$  in  $\bar{v}$ , and the strengths  $\beta_p$  for  $p=2-8$ . In practice, the number of  $\beta_p$  parameters is reduced by assuming that

$$\beta_\tau = \beta_{\sigma\tau} = \beta_b = \beta_{b\tau} = \beta_\sigma \quad (2.24)$$

and

$$\beta_{t\tau} = \beta_t. \quad (2.25)$$

In variational calculations of few-body nuclei, it has proven beneficial to modify the  $U_{ij}$  by a product of three-body correlation factors [17]:

$$U_{ij} \rightarrow \prod_{k \neq i,j} f_3(r_{ij}; r_{ik}, r_{jk}) U_{ij}, \quad (2.26)$$

$$f_3(r_{ij}; r_{ik}, r_{jk}) = 1 - t_1 \left[ \frac{r_{ij}}{R_{ijk}} \right]^{t_2} \exp(-t_3 R_{ijk}), \quad (2.27)$$

$$R_{ijk} = r_{ij} + r_{ik} + r_{jk}. \quad (2.28)$$

The functions  $f_3(r_{ij}; r_{ik}, r_{jk})$  reduce the spin-isospin correlations of nucleons  $i$  and  $j$  when a third nucleon  $k$  comes close to both. This modification of  $U_{ij}$  is also used in the present study of  $^{16}\text{O}$ , and it contains the variational parameters  $t_1$ ,  $t_2$ , and  $t_3$ .

The  $U_{ijk}$  is meant to represent the triplet correlations induced by the three-nucleon interaction  $V_{ijk}$ . The form

$$U_{ijk} = \varepsilon \tilde{V}_{ijk}, \quad (2.29)$$

suggested by perturbation theory, is used. Here  $\tilde{V}_{ijk}$  is the same as  $V_{ijk}$  [Eqs. (2.5)–(2.7)], except for the range  $b'$  of the cutoff function in  $Y_\pi(r)$  and  $T_\pi(r)$ :

$$Y_\pi(r) = (1 - e^{-b'r^2})e^{-x}/x, \quad (2.30)$$

$$T_\pi(r) = \left[ 1 + \frac{3}{x} + \frac{3}{x^2} \right] (1 - e^{-b'r^2}) Y_\pi(r), \quad (2.31)$$

$$x = \mu_\pi r. \quad (2.32)$$

The parameters  $\varepsilon$  and  $b'$  are determined variationally.

In nuclei with  $A \leq 5$ , only the terms linear in  $U_{ijk}$  have been kept in the calculation of the wave function. This corresponds to using an "independent-triplet" (IT) product of  $1 + U_{ijk}$  in the variational wave function. The IT product is defined like the independent-pair (IP) product [18],

$$\prod_{\text{IT}} (1 + U_{ijk}) = 1 + \sum_{i < j < k} U_{ijk} + \frac{1}{2} \sum_{\substack{i < j < k \\ i' < j' < k' \neq i, j, k}} U_{ijk} U_{i'j'k'} + \dots, \quad (2.33)$$

and it is much simpler to use. Approximating the symmetrized product of  $1 + U_{ij}$  by an IP product has a relatively small effect on the energies of few-body nuclei, and hence the IT product of  $1 + U_{ijk}$  could be an excellent approximation.

### III. CLUSTER EXPANSION

We wish to evaluate expectation values of various operators for trial functions of the form given by Eq.

(2.9). In particular, we need to evaluate the energy expectation value

$$E_v = \frac{\langle \Psi_v | H | \Psi_v \rangle}{\langle \Psi_v | \Psi_v \rangle} \geq E_0 \quad (3.1)$$

and vary  $\Psi_v$  to minimize it. The optimum  $\Psi_v$  can then be used to evaluate other quantities of interest.

Evaluation of expectation values with the  $\Psi_v$  is numerically difficult because of the summation over the discrete spin and isospin indices. The  $\Psi_v$  can be represented as a vector of

$$N = 2^A \begin{bmatrix} A \\ Z \end{bmatrix} \quad (3.2)$$

spin-isospin components  $\psi_n(\mathbf{R})$ , where  $\mathbf{R} = (\mathbf{r}_1, \dots, \mathbf{r}_A)$  is a given spatial configuration; the  $\psi_n$  are the amplitudes of states with definite  $\sigma_z$  and  $\tau_z$  for each nucleon. The large noncentral operators in the nuclear interaction can produce significant contributions from relatively small  $\psi_n$ . The number  $N$  grows very rapidly with  $A$  and  $Z$ , e.g.,  $N = 24, 96, 1280$ , and  $843\,448\,320$  for  ${}^3\text{H}$ ,  ${}^4\text{He}$ ,  ${}^6\text{Li}$ , and  ${}^{16}\text{O}$ , respectively. Monte Carlo (MC) integration methods [17] have been developed for use in few-body nuclei that sample the spatial configuration  $\mathbf{R}$  and order of operators in the symmetrized product of Eq. (2.9) while performing a complete summation over the  $N$  discrete spin-isospin components. However, this complete summation becomes impossibly expensive for  $A > 8$ .

The  $3(A-1)$ -dimensional spatial integration implied

in the expectation value (3.1) does not pose any serious difficulty in a MC calculation. For example, VMC calculations of drops of Fermi-liquid  ${}^3\text{He}$  atoms with  $A \leq 240$  have been performed [19]. These calculations were possible because the interaction between  ${}^3\text{He}$  atoms is independent of spin, and hence one can assign particles 1 to  $A/2$  to be spin up and particles  $A/2+1$  to  $A$  to be spin down; these assignments persist because the correlations and interactions do not flip spins.

We can expand the  $\langle \Psi_v | H | \Psi_v \rangle$  and  $\langle \Psi_v | \Psi_v \rangle$  according to the number of nucleons connected by the spin-isospin correlations  $U_{ij}$  and  $U_{ijk}$  and obtain a cluster expansion for  $E_v$ . This cluster expansion is probably much better behaved than the conventional expansions [20] because it treats exactly all the exchanges and central correlations between the  $A$  nucleons. In the conventional cluster expansions, one also expands in powers of  $f_c^2(r) - 1$  and does not necessarily keep all exchange terms. The present cluster expansion is obtained by following the methods developed in Ref. [20] for nuclear matter. However, there are many significant differences as discussed below.

Because there are many ways of partitioning the  $A$  nucleons into four groups of  $A/4$  nucleons, the  $|\Psi_J\rangle$  and  $|\Psi_v\rangle$  contain a very large number of terms. However, since  $H$  is a symmetric operator,

$$E_v = \frac{\langle \Psi_v | H | \Psi_R \rangle}{\langle \Psi_v | \Psi_R \rangle}, \quad (3.3)$$

where  $|\psi_R\rangle$  is not fully antisymmetric; it is defined as

$$|\Psi_R\rangle = \left[ \prod_{\text{IT}} (1 + U_{ijk}) \right] \left[ \mathcal{S} \prod_{i < j} (1 + U_{ij}) \right] \left[ \prod_{i < j} f_c(r_{ij}) \right] |\Phi\rangle, \quad (3.4)$$

without the  $\mathcal{A}$  in  $\Psi_v$  of Eqs. (2.9) and (2.10).

Consider, for example, the expectation value of a symmetric one-body operator:

$$\frac{\langle \Psi_v | \sum_i O_i | \Psi_R \rangle}{\langle \Psi_v | \Psi_R \rangle} = \frac{N}{D}. \quad (3.5)$$

The  $N$  and  $D$  can be expanded as a sum of  $n$ -body contributions:

$$N = \sum_i n_i + \sum_{i < j} n_{ij} + \sum_{i \neq j < k} n_{i,jk} + \sum_{i < j < k} n_{ijk} + \dots + n_{12 \dots A}, \quad (3.6)$$

$$D = 1 + \sum_{i < j} d_{ij} + \sum_{i < j < k} d_{ijk} + \sum_{\substack{i < j \neq k < l \\ i < k}} d_{ij,kl} + \dots + d_{12 \dots A}. \quad (3.7)$$

The expectation value  $\langle X \rangle$  is defined as

$$\langle X \rangle = \frac{\langle \Phi | \mathcal{A} \left[ \prod_{i < j} f_c(r_{ij}) \right] X \left[ \prod_{i < j} f_c(r_{ij}) \right] | \Phi \rangle}{\langle \Phi | \left[ \prod_{i < j} f_c(r_{ij}) \right]^2 | \Phi \rangle}, \quad (3.8)$$

and the contributions  $n_{ij} \dots$  and  $d_{ij} \dots$  are obtained as

$$n_i = \langle O_i \rangle, \quad (3.9)$$

$$n_{ij} = \langle (1 + U_{ij}^\dagger)(O_i + O_j)(1 + U_{ij}) \rangle - n_i - n_j, \quad (3.10)$$

$$n_{i,jk} = \langle (1 + U_{jk}^\dagger)O_i(1 + U_{jk}) \rangle - n_i, \quad (3.11)$$

$$n_{ijk} = \left\langle \left[ \prod_{\text{cyc}} (1 + U_{ij}^\dagger) \right] (1 + U_{ijk}^\dagger) (O_i + O_j + O_k) (1 + U_{ijk}) \left[ \prod_{\text{cyc}} (1 + U_{ij}) \right] \right\rangle - \sum_{\text{cyc}} (n_{i,jk} + n_{ij} + n_i), \quad (3.12)$$

$$d_{ij} = \langle (1 + U_{ij}^\dagger)(1 + U_{ij}) \rangle - 1, \quad (3.13)$$

etc. In the CMC method developed in the present work, the expectation values  $n_i, n_{ij}, \dots$  and  $d_{ij}, d_{ijk}, \dots$  are calculated. The operators in the expectation value  $n_{ij \dots l}$  or  $d_{ij \dots l}$  contain only the spin and isospin of the particles  $ij \dots l$ . The spins and isospins of the other particles are unchanged and hence can be essentially ignored. If  $ij \dots l$  are in a single determinant  $D_{\sigma\tau}$  in  $|\Phi\rangle$ , only the term  $\langle \Phi |$  in  $\langle \Phi | \mathcal{A}$  contributes and the rest can be ignored. If  $i$  is in  $D_{\sigma'\tau'}$  and  $j \dots l$  are in  $D_{\sigma\tau}$  in  $|\Phi\rangle$ , then we need to consider only the direct term  $\langle \Phi |$  and those obtained by exchanging  $i$  with  $j \dots l$  in  $\langle \Phi | \mathcal{A}$ . For these reasons it appears possible, with currently available computers, to calculate expectation values  $n_{ij \dots l}$  and  $d_{ij \dots l}$  containing up to five nucleons, though in the present calculation we stop at four-body terms. We again emphasize that every term in the cluster expansion contains

$$c_i = n_i, \quad (3.16)$$

$$c_{ij} = \frac{n_{ij} - (c_i + c_j)d_{ij}}{1 + d_{ij}}, \quad (3.17)$$

$$c_{i,jk} = \frac{n_{i,jk} - c_i d_{jk}}{1 + d_{jk}}, \quad (3.18)$$

$$c_{ijk} = \frac{n_{ijk} - \sum_{\text{cyc}} [c_i d_{ijk} + (c_{ij} + c_{k,ij})(d_{ik} + d_{jk} + d_{ijk})]}{1 + \sum_{\text{cyc}} d_{ij} + d_{ijk}}, \dots \quad (3.19)$$

Terms of type  $c_{i,jk}, c_{ij,kl}, \dots$  do not appear in the conventional cluster expansions in which one defines an  $h_{ij}$  such that

$$(1 + U_{ij})f_c(r_{ij}) = 1 + h_{ij}. \quad (3.20)$$

The conventional expansions are similar to the present except that the  $U_{ij}$  get replaced by  $h_{ij}$  and the expectation values, denoted by  $\langle X \rangle$  in Eq. (3.8), do not contain products of the  $f_c$ 's. In this case,  $n_{i,jk}$  [Eq. (3.11)] contains two disconnected integrals  $n_i$  and  $d_{jk}$ , and hence  $c_{i,jk} = 0$ . Because of the products of  $f_c(r_{ij})$  in all the expectation values, there are no disconnected diagrams in the present expansion; terms such as  $c_{i,jk}$  are small because of large cancellation between  $n_{i,jk}$  and  $c_i d_{jk}$ , but they are finite. They represent parts of contributions of clusters with more than three nucleons in the conventional expansions. We will refer to these terms as semifactorizable.

The  $|\Phi\rangle$  is a product of four determinants in which particles 1-4, 5-8, 9-12, and 13-16 are, respectively,  $p\uparrow, p\downarrow, n\uparrow$ , and  $n\downarrow$ , while  $\langle \Phi | \mathcal{A}$  is fully antisymmetric. Thus the expectation values

$$n_{ij \dots l} = n_{i'j' \dots l'}, \quad (3.21)$$

the complete product of central correlations and hence is a  $3(A-1)$ -dimensional integral.

The expansions (3.6) and (3.7) for  $N$  and  $D$  are divergent. Convergent linked cluster expansions

$$\frac{\langle \Psi_v | \sum_i O_i | \Psi_R \rangle}{\langle \Psi_v | \Psi_R \rangle} = \sum_i c_i + \sum_{i < j} c_{ij} + \sum_{i \neq j < k} c_{i,jk} + \sum_{i < j < k} c_{ijk} + \dots \quad (3.14)$$

are obtained from the equation

$$\left[ \sum_i c_i + \sum_{i < j} c_{ij} + \dots \right] D = N \quad (3.15)$$

by equating terms that contain the same particles:

$$d_{ij \dots l} = d_{i'j' \dots l'}, \quad (3.22)$$

when  $i$  and  $i'$  belong to the same determinant. In MC calculations we can average over these identical expectation values to reduce sampling errors. For example,  $A(A-1)/2$  values of  $n_{ij}$  ( $i < j$ ) are calculated, but in a nucleus such as  $^{16}\text{O}$ , in which  $N=Z$  and the effects of the Coulomb potential on the wave function are neglected, there are only four different  $n_{ij}$ 's:

$$n_{p\uparrow p\uparrow} = n_{p\downarrow p\downarrow} = n_{n\uparrow n\uparrow} = n_{n\downarrow n\downarrow}, \quad (3.23)$$

$$n_{p\uparrow p\downarrow} = n_{n\uparrow n\downarrow}, \quad (3.24)$$

$$n_{p\uparrow n\uparrow} = n_{p\downarrow n\downarrow}, \quad (3.25)$$

$$n_{p\uparrow n\downarrow} = n_{p\downarrow n\uparrow}. \quad (3.26)$$

The above equations present a general framework to expand  $E_v$ . We have considered three different expansions which differ only in the treatment of the antisymmetrization. In the first cluster expansion, called CEA, we use the average values of  $n_{\sigma_i \tau_i, \sigma_j \tau_j \dots}$  and  $d_{\sigma_i \tau_i, \sigma_j \tau_j \dots}$  to obtain the cluster contributions. The  $c_{ij \dots}$  also depend only upon  $\sigma_i \tau_i, \sigma_j \tau_j \dots$  and may be considered as  $c_{\sigma_i \tau_i, \sigma_j \tau_j \dots}$ .

The second cluster expansion, called CEB, has the following motivation. The expectation values  $\bar{n}_{ij\dots l}$  and  $\bar{d}_{ij\dots l}$  calculated with the full  $\mathcal{A}|\Phi\rangle$ , in place of  $|\Phi\rangle$  in Eq. (3.8), do not depend upon the particle numbers  $ij\dots l$ . In fact, they are given by the average of  $n_{ij\dots l}$  and  $d_{ij\dots l}$ , respectively, over all  $ij\dots l$ . For example,

$$\bar{n}_{ij} = \frac{2}{A(A-1)} \sum_{i' < j'} n_{i'j'} . \quad (3.27)$$

In CEB the cluster contributions are calculated with the  $\bar{n}$  and  $\bar{d}$ .

Every cluster contribution of CEA or CEB retains the effect of spatial correlations  $f_c(r_{ij})$  and exchanges between all the  $A$  nucleons in the nucleus. This can be rather easily achieved since the  $\prod f_c(r_{ij})$  and the determinants can be very efficiently computed. Most of the computation effort in the present calculations goes into evaluating the matrix elements of the products of spin, isospin, and tensor operators in  $U_{ij}$  and  $U_{ijk}$ .

The third cluster expansion, called CEC, is obtained by keeping only the exchanges between particles  $ij\dots l$  in the evaluation of  $d_{ij\dots l}$  and  $n_{ij\dots l}$ . The CEC expectation values are defined as

$$\langle X \rangle = \frac{\langle \Phi_p | \mathcal{A}' \left[ \prod_{i < j} f_c(r_{ij}) \right] X \left[ \prod_{i < j} f_c(r_{ij}) \right] | \Phi_p \rangle}{\langle \Phi_p | \left[ \prod_{i < j} f_c(r_{ij}) \right]^2 | \Phi_p \rangle} , \quad (3.28)$$

$$\Phi_p = \phi_1(x_1) \phi_2(x_2) \cdots \phi_A(x_A) , \quad (3.29)$$

$$x_i = \mathbf{r}_i, \sigma_i, \tau_i , \quad (3.30)$$

and the antisymmetrization operator  $\mathcal{A}'$  includes only the exchanges between particles  $ij\dots l$  that appear in  $X$ . In CEC we use the average values  $\bar{n}_{ij\dots l}$  and  $\bar{d}_{ij\dots l}$  to obtain the cluster contributions.

The CEB is the linked cluster expansion of the expectation value (3.1), while CEA is that for the expectation value (3.3). Even though these expectation values are identical, their cluster expansions are different. The CEC is yet another expansion of (3.1). Thus, by comparing the results obtained with CEA, CEB, and CEC, we hope to learn about their convergence.

So far, we have discussed the cluster expansion for the expectation value of the sum of one-body operators. Those for the expectation value of the sum of two- or three-body operators such as  $v_{ij}$  and  $V_{ijk}$  are very similar. In the case of that for a sum of  $v_{ij}$ , there are no one-body terms  $n_i$ , nor terms such as  $n_{i,jk\dots}$  in  $N$  [Eq. (3.6)]. Hence the cluster expansion contains only the terms  $c_{ij}, c_{ijk}, c_{ij,kl}, c_{ijkl}, \dots$ . Similarly, that for the sum of  $V_{ijk}$  contains the terms  $c_{ijk}, c_{ijkl}, c_{ijk,lm}, c_{ijklm}, \dots$ .

It is not necessary to treat the semifactorizable terms separately from the others. For example, we can define cluster contributions  $\bar{c}_{ij\dots k}$  as the sum of all those that contain particles  $ij\dots k$ , so that

$$\bar{c}_{ijk} = c_{ijk} + c_{i,jk} + c_{j,ik} + c_{k,ij} , \quad (3.31)$$

etc. The corresponding  $\bar{n}_{ijk}, \bar{n}_{ijkl}$  can also be directly

computed without separating their semifactorizable contributions.

The total  $n$ -body cluster contribution  $C_n$  to the expectation value is obtained from the sum

$$C_n = \sum_{i_1 < i_2 < \dots < i_n} \bar{c}_{i_1 i_2 \dots i_n} , \quad (3.32)$$

which includes the semifactorizable terms. The semifactorizable terms give large contributions to the Monte Carlo variance of  $\bar{c}_{ij\dots k}$ . They are, however, much easier to calculate, and so, in order to calculate the  $n$ -body cluster contribution in an optimum fashion, it is efficient to sample the semifactorizable terms more often than the others. In order to get comparable contributions from  $c_{ijkl}$  and the semifactorizable terms to the sampling error of  $C_4$ , four times more configurations were needed in the present work to calculate the four-body semifactorizable terms.

The statistical errors in  $C_1, C_2, C_3$ , and  $C_4$  are correlated because the contributions of larger clusters are obtained by subtracting those of the smaller subclusters via Eqs. (3.10)–(3.12) and (3.17)–(3.19). Therefore the variance in the sum  $C_1 + C_2 + C_3 + C_4$  is smaller, often by a factor of 3, than that in the uncorrelated sum, in which different configurations are used to calculate the various  $C_n$ . Hence it is advantageous to use the same configurations to calculate the sum of  $C_n$ . For this reason, separating the semifactorizable contributions does not appear to be essential in  $^{16}\text{O}$  if the only quantity of interest is the sum of  $C_n$ . However, in larger nuclei it may be advantageous to separate their contribution to all quantities of interest.

#### IV. CALCULATIONAL METHODS

The  $3(A-1)$ -dimensional integrals in Eq. (3.8) are calculated with MC techniques [21] using a Metropolis random walk. In this method,

$$\frac{\int d\mathbf{R} W(\mathbf{R}) I(\mathbf{R})}{\int d\mathbf{R} W(\mathbf{R})} = \lim_{N_c \rightarrow \infty} \frac{1}{N_c} \sum_{i=1, N_c} I(\mathbf{R}_i) . \quad (4.1)$$

Here  $N_c$  is the number of configurations  $\mathbf{R}_i$  chosen with probability proportional to  $W(\mathbf{R})$ , and  $\mathbf{R}$  represents the particle coordinates  $\mathbf{r}_1, \mathbf{r}_2, \dots, \mathbf{r}_A$ , with the constraint  $\mathbf{R}_{\text{c.m.}} = 0$ . The weight function  $W(\mathbf{R})$  has to be chosen such that it is positive and normalizable, and the variance of  $I(\mathbf{R}_i)$  is as small as possible. In practice, one must use a finite number  $N_c$  of configurations, and then the statistical error in the MC calculation is given by  $\sqrt{\text{var}/N_c}$ .

In the present calculations, we have used

$$W(\mathbf{R}) = \Phi^*(\mathbf{R}) \left[ \prod_{i < j} f_c(r_{ij}) \right]^2 \Phi(\mathbf{R}) F(\mathbf{R}) , \quad (4.2)$$

so that the expectation value  $\langle X \rangle$  of Eq. (3.8) is given by

$$\langle X \rangle = \frac{\int d\mathbf{R} W(\mathbf{R}) \Phi^*(\mathbf{R}) \mathcal{A} X \Phi(\mathbf{R}) / \Phi^*(\mathbf{R}) \Phi(\mathbf{R}) F(\mathbf{R})}{\int d\mathbf{R} W(\mathbf{R}) / F(\mathbf{R})} . \quad (4.3)$$

Note that  $\mathcal{A}$  and  $X$  are operators, spin-isospin summations are implicit in  $\Phi^*(\mathbf{R})\mathcal{A}X\Phi(\mathbf{R})$ , and in the present case  $\Phi(\mathbf{R})$  is real so that  $\Phi^*=\Phi$ . The numerator and denominator of Eq. (4.3) are both evaluated in the same Metropolis walk controlled by  $W(\mathbf{R})$ .

The  $\Phi(\mathbf{R})$ , being a product of four determinants [Eq. (2.13)], can be small in certain regions of  $\mathbf{R}$ . However,  $\Phi^*(\mathbf{R})\mathcal{A}$  is a sum of products of determinants which is not necessarily small where  $\Phi(\mathbf{R})$  is small. For example, when  $\mathbf{r}_1 \sim \mathbf{r}_2$ ,  $\Phi(\mathbf{R})$  is small because nucleons 1 and 2 are  $p \uparrow$  in  $\Phi(\mathbf{R})$ . However,  $\Phi^*(\mathbf{R})\mathcal{A}$  has terms in which 1 and 2 have different spin and isospin, and these may be large even when  $\mathbf{r}_1 \sim \mathbf{r}_2$ . The quantity  $\Phi^*(\mathbf{R})\mathcal{A}X\Phi(\mathbf{R})/|\Phi(\mathbf{R})|^2$  can become very large in such regions and, thus, has a large variance.

The factor  $F(\mathbf{R})$  in the  $W(\mathbf{R})$  is meant to avoid this problem, and it was chosen so that  $\Phi^*(\mathbf{R})\mathcal{A}X\Phi(\mathbf{R})/|\Phi(\mathbf{R})|^2F(\mathbf{R})$  is finite at all  $\mathbf{R}$ . All exchanges that may contribute to  $\Phi^*(\mathbf{R})\mathcal{A}X\Phi(\mathbf{R})$  are included in  $|\Phi(\mathbf{R})|^2F(\mathbf{R})$  so that

$$\begin{aligned} & |\Phi(\mathbf{R})|^2F(\mathbf{R}) \\ &= |\Phi(\mathbf{R})|^2 + \sum_{i < j} \omega(r_{ij}) |P_{ij}\Phi(\mathbf{R})|^2 \\ &+ \sum_{i < j < k} \omega(r_{ij})\omega(r_{jk})\omega(r_{ik}) \\ &\quad \times \{ |P_{ij}P_{ik}\Phi(\mathbf{R})|^2 + |P_{ik}P_{ij}\Phi(\mathbf{R})|^2 \} + \dots \end{aligned} \quad (4.4)$$

In a calculation meant to evaluate all  $m \leq n$  body clusters, only the terms with  $\leq n$ -body exchanges need to be considered in  $|\Phi(\mathbf{R})|^2F(\mathbf{R})$ . Further, the sums in Eq. (4.4) can be restricted to only those  $ij \dots$  that are in different determinants in  $\Phi$ . The function  $\omega(r)$  can be chosen conveniently; we have used  $\omega(r)$  proportional to the sum of the squares of  $u_p(r)$ , since the exchange of particles  $i$  and  $j$  with different spin-isospin states in  $\Phi$  must be accompanied by a  $v_{ij}$ ,  $U_{ij}$ ,  $V_{ijk}$ , or  $U_{ijk}$ .

There are 120 pairs of nucleons in  $^{16}\text{O}$  and hence the symmetrization operator  $\mathcal{S}$  in  $\Psi_v$  and  $\Psi_R$  introduces 120! orderings of the  $1+U_{ij}$  in the expectation value (3.3). This sum of the orderings of  $1+U_{ij}$  is sampled by choosing two random orderings of the 120 pairs, one for  $\Psi_v$  and the other for  $\Psi_R$ , at each configuration  $\mathbf{R}_i$ .

The  $\Phi^*(\mathbf{R})\mathcal{A}X\Phi(\mathbf{R})$  for a given cluster is calculated with methods developed for few-body nuclei [3,17,22]. The terms in  $\Phi^*(\mathbf{R})\mathcal{A}$  that can contribute are summed, and  $\Phi^*(\mathbf{R})\mathcal{A}$  is represented as a vector whose components give the amplitudes of the spin-isospin states of the nucleons in the cluster. The corresponding vector representing  $\Phi(\mathbf{R})$  has only one nonzero component since all particles have definite values of  $\sigma_z$  and  $\tau_z$  in  $\Phi(\mathbf{R})$ . The  $v_{ij}$ ,  $V_{ijk}$ ,  $U_{ij}$ , and  $U_{ijk}$  operate on these vectors as discussed in Refs. [3], [17], and [22]. The expectation values of the kinetic-energy operators are obtained by computing  $\Psi_R$  at slightly shifted positions and using finite differences to evaluate terms in  $\nabla_i^2\Psi_R$ .

In a two-proton, two-neutron, four-body cluster, the vector representing  $\prod(1+U_{ij})\Phi(\mathbf{R})$  or  $\prod(1$

$+U_{ij})\mathcal{A}\Phi(\mathbf{R})$  generally has 96 nonzero components. In contrast, the vector representing  $\Phi(\mathbf{R})$  has only one, and that for  $\mathcal{A}\Phi(\mathbf{R})$  has at most 24 nonzero components. All the possible 96 components of the vector get filled by successive operations with the  $U_{ij}$ 's. Hence it is more efficient, by a factor of  $\sim 2.3$ , to use the wave functions

$$\begin{aligned} |\tilde{\Psi}_R\rangle &= \left[ \mathcal{S} \prod_{i < j} (1+U_{ij}) \right] \left[ \prod_{\text{IT}} (1+U_{ijk}) \right] \\ &\quad \times \left[ \prod_{i < j} f_c(r_{ij}) \right] |\Phi\rangle \end{aligned} \quad (4.5)$$

and the corresponding  $|\tilde{\Psi}_v\rangle$ , rather than the  $|\Psi_v\rangle$  and  $|\Psi_R\rangle$  given by Eqs. (2.9) and (3.4). In  $\tilde{\Psi}_R$  and  $\tilde{\Psi}_v$ , the  $U_{ijk}$ 's operate on the sparse vectors representing  $\Phi(\mathbf{R})$  and  $\mathcal{A}\Phi(\mathbf{R})$ .

The perturbative arguments [23] used to model the  $U_{ijk}$  assume that the  $\prod(1+U_{ijk})$  is to the left of the  $\prod(1+U_{ij})$ . Nevertheless, the  $\Psi_v$  and  $\tilde{\Psi}_v$  are not too different, and hence we determine the variational parameters by minimizing the energy  $\tilde{E}_v$  calculated with  $\tilde{\Psi}_v$ . In the end the small difference between  $E_v$  and  $\tilde{E}_v$  is calculated in a single random walk. In the search for optimum variational parameters, differences between the energies given by a set of  $\Psi_v$  are used. These energy differences can be calculated in a single walk with much smaller statistical errors [3,21,22].

The numerical evaluation of  $\nabla_i^2\Psi_v$ , required to calculate the kinetic energy, is the most time-consuming part of the present calculation. The calculation of the contribution of many-body clusters to the kinetic energy becomes particularly difficult when the spin-orbit correlations  $u_{b,b\tau}$  are included in the  $U_{ij}$ . Fortunately, the interactions  $v_p(r_{ij})O_{ij}^p$ ,<sup>7,14</sup> together with the  $u_{b,b\tau}$  correlations give a rather small contribution to  $E_v$ . It is, however, necessary to retain the  $u_{b,b\tau}$  correlations in the calculation of  $v_{b,b\tau}$  interaction contributions.

In order to calculate  $E_v$  efficiently, we define  $H_6$  and  $\Psi_{6,v}$  as

$$H_6 = T + \sum_{i < j} \left[ \sum_{p=1,6} v_p(r_{ij})O_{ij}^p + v_{\text{Coul}}(r_{ij}) \right] + V, \quad (4.6)$$

$$\Psi_{6,v} = \left[ \prod_{\text{IT}} (1+U_{ijk}) \right] \left[ \mathcal{S} \prod_{i < j} (1+U'_{ij}) \right] \left[ \prod_{i < j} f_c(r_{ij}) \right] \mathcal{A}\Phi, \quad (4.7)$$

$$U'_{ij} = \prod_{k \neq i,j} f_3(r_{ij}; r_{jk}, r_{ik}) \left[ \sum_{p=2,6} \beta_p u_p(r_{ij})O_{ij}^p \right], \quad (4.8)$$

and  $\Psi_{6,R}$ ,  $\tilde{\Psi}_{6,v}$ , and  $\tilde{\Psi}_{6,R}$  are also defined analogously. Contributions of up to four-body clusters to the energy

$$E_{6,v} = \frac{\langle \Psi_{6,v} | H_6 | \Psi_{6,R} \rangle}{\langle \Psi_{6,v} | \Psi_{6,R} \rangle} \quad (4.9)$$

are calculated, and the small difference

$$\Delta E_{p>6} = E_v - E_{6,v} \quad (4.10)$$

is estimated from two-body clusters alone.

The statistical error  $\sigma$  in the average of  $N$  samples,  $s_n$ , with normal distribution, is given by

$$\sigma = \left\{ \frac{1}{N} \left[ \frac{1}{N} \sum_{n=1, N} s_n^2 - \left( \frac{1}{N} \sum_{n=1, N} s_n \right)^2 \right] \right\}^{1/2}. \quad (4.11)$$

This equation can be used to estimate the sampling error in the calculated values of the  $n_{ij\dots}$  and  $d_{ij\dots}$ . The cluster contributions  $c_{ij\dots}$  [Eqs. (3.16)–(3.19)] are ratios of sums of products of the  $n$ 's and  $d$ 's, and in order to estimate the error in their calculation, we need to compute the correlation coefficients between the  $n$ 's and  $d$ 's. This is avoided by using the following approximate method.

After every  $m$  steps of the random walk, the cluster contributions are calculated using running averages of the  $n$ 's and  $d$ 's. This produces a sequence of improving estimates  $[c_{ij\dots}]_n$ ,  $n=1, N$ , where  $N=N_c/m$ . We then define

$$\{c_{ij\dots}\}_1 = [c_{ij\dots}]_1, \quad (4.12)$$

$$\{c_{ij\dots}\}_n = n[c_{ij\dots}]_n - (n-1)[c_{ij\dots}]_{n-1}. \quad (4.13)$$

The result  $[c_{ij\dots}]_N$  of the calculation is just the average value of the  $\{c_{ij\dots}\}_n$ ,  $n=1, \dots, N$ . If the  $c_{ij\dots}$  were linear functions of the  $n$ 's and  $d$ 's, the  $\{c_{ij\dots}\}_n$  would be independent block-averaged samples of  $c_{ij\dots}$ , and the error would be given by Eq. (4.11) if the block size  $m$  is chosen large enough so that  $\{c_{ij\dots}\}_n$  have a normal distribution. In reality, the  $c_{ij\dots}$  are linear functions of the  $n_{ij\dots}$ , but not of the  $d$ 's. However, the variance of the  $d$ 's is much smaller than that of the  $n$ 's, and hence the error estimates obtained from the  $\{c_{ij\dots}\}_n$  are very reliable. The statistical errors reported in this paper are estimated from the  $\{c_{ij\dots}\}_n$  using  $m \sim 10$ – $20$ . We have verified that these error estimates are accurate for the two-body cluster contributions from detailed calculations of the correlated error in  $c_{ij}$ .

If the cluster expansions are summed all the way up to the maximum possible  $A$ -body cluster contribution, then the result will be an exact evaluation of  $E_v$ . We have done this for the case of  ${}^4\text{He}$  and compared the results

with a completely independent Monte Carlo calculation of  $E_v$  without cluster expansion [3]. The two calculations agree to within the statistical errors of  $\lesssim 1\%$ .

The  ${}^{16}\text{O}$  calculations were carried out on a single processor of a Cray-2 computer running at an average speed of just over 100 MFLOPS. The CPU times per configuration required to calculate the three- and four-body cluster contributions to  $\bar{E}_{6,v}$  with  $\bar{\Psi}_{6,v}$  are 0.56 and 15 s, respectively. Of this, 0.41 and 11 s are used to calculate kinetic-energy contributions. Evaluation of the two-body cluster contribution to  $\Delta E_{p>6}$  takes only 0.13 s per configuration. Searches for optimal values of the variational parameters used  $\sim 500$ – $1000$  configurations, while  $\sim 5000$  configurations are needed to have a statistical error  $\sim 0.2$  MeV/nucleon for the total energy. The calculation of  $E_v - \bar{E}_v$  takes  $\sim 10$  CPU hours.

Most of the computational effort goes into evaluating the products of  $U_{ij}$ 's and  $U_{ijk}$ 's operating on the  $|\Phi\rangle$  and  $\mathcal{A}|\Phi\rangle$ . This part is identical in the cluster expansions CEA, CEB, and CEC. Hence the required computer time per configuration is rather similar for these three expansions; the additional calculations of the determinants in CEA and CEB take relatively negligible time.

## V. COMPARISON OF THE CLUSTER EXPANSIONS

In this section we compare the convergence and MC variance of the three cluster expansions defined in Sec. III. All the results shown here are for  $\bar{E}_{6,v}$  calculated from the  $\bar{\Psi}_{6,v}$  with optimum variational parameters. The results for total  $E_v$  including the  $\Delta E_{p>6}$  and  $E_v - \bar{E}_v$  are presented in the next section.

The calculated cluster contributions in CEA, CEB, and CEC are shown in Table I. For brevity, we use  $T$ ,  $v_6$ ,  $V^{2\pi}$ , and  $V^R$  to denote expectation values of the kinetic energy, the  $p \leq 6$  terms in  $v_{ij}$  and the Coulomb interaction, and the three-nucleon interactions  $V_{ijk}^{2\pi}$  and  $V_{ijk}^R$ . Also,  $n$ -body cluster contributions to these quantities are

TABLE I. Cluster contributions to  $\bar{E}_{6,v}$  of  ${}^{16}\text{O}$  in MeV/nucleon.

		1b	2b	3b	4b	5-16b	Sum
$T$	CEA	18.8	16.5	-1.2	-0.3(2) <sup>a</sup>	$\sim 0$	33.7
	CEB	18.8	16.7	-1.6	-0.2(2)	$\sim 0$	33.8(2)
	CEC	18.8	14.8	0.1(2)	0.2(1.2)	$\sim 0$	33.8(1.2)
$v_6$	CEA		-45.3	6.7	-0.1(2)	$\sim 0$	-38.4
	CEB		-45.8	7.7	-0.7(2)	$\sim 0$	-38.8(2)
	CEC		-42.1	2.6	0.1(5)	$\sim 0$	-39.4(5)
$V^{2\pi}$	CEA			-6.2	2.8	-0.8	-4.3
	CEB			-6.4	3.1	-1.0	-4.3
	CEC			-5.1	0.8	-0.1	-4.4
$V^R$	CEA			2.6	-0.6	0.1	2.1
	CEB			2.7	-0.7	0.1	2.1
	CEC			2.2	0.0	0.0	2.2
$\bar{E}_{6,v}$	CEA	18.8	-28.8	1.9	1.8	-0.7	-7.0(1)
	CEB	18.8	-29.1	2.4	1.5	-0.9	-7.2(1)
	CEC	18.8	-27.3	-0.2(2)	1.1(8)	-0.1	-7.7(8)

<sup>a</sup>The Monte Carlo sampling errors are shown in parenthesis only when they exceed 0.1 MeV/nucleon.



denoted by  $T(nb)$ , etc. The sum of  $V^{2\pi}$  and  $V^R$  is denoted by  $V$ , while  $\bar{E}_{6,v}$  is the sum of  $T$ ,  $v_6$ , and  $V$ . The columns give cluster contributions and their sums. The four-body cluster contributions are dominated by the three-nucleon interactions, particularly by the long-range  $V_{ijk}^{2\pi}$ . Note that some of the  $T(4b)$  and  $v_6(4b)$  are statistically consistent with zero.

The statistical errors due to MC sampling of the cluster contributions in 10000 configurations are shown in Table II. The errors are strongly correlated; that in the cluster contributions to  $\bar{E}_{6,v}$  is much less than the sum of the errors in  $T$ ,  $v_6$ , and the total  $V$ . This is to be expected; when  $\Psi$  is close to an eigenstate of  $H$ , the fluctuations in  $T\Psi$ ,  $v\Psi$ , and  $V\Psi$  essentially cancel each other. The smallest sampling error is in the sum of one- to four-body cluster contributions to the expectation value  $\bar{E}_{6,v}$  of  $H_6$ . This is particularly nice because  $\bar{E}_{6,v}$  is the quantity of primary interest in the variational calculation.

The convergence of CEA and CEB is similar, while that of CEC is significantly better, particularly for  $V^{2\pi}$ . Let  $c_{ijk}$  be a three-body cluster contributing to  $V^{2\pi}(3b)$ ; it contains terms having  $V_{ijk}^{2\pi}$  and any or all of  $U_{ij}$ ,  $U_{ik}$ ,  $U_{jk}$ , and  $U_{ijk}$  in all the cluster expansions. However, in CEC only those terms having exchanges among  $i$ ,  $j$ , and  $k$  are included in  $c_{ijk}$ , while in CEA and CEB the terms in which  $i$ ,  $j$ , and/or  $k$  are exchanged with the other nucleons in the nucleus are also included in  $c_{ijk}$ . These extra exchanges seem to give a negative contribution which makes  $V^{2\pi}(3b)$  more negative in CEA and CEB than in CEC. The  $V^{2\pi}(4b)$  is positive in all cluster expansions; however, it is smallest in CEC because it contains some of the negative contributions that are a part of  $V^{2\pi}(3b)$  in CEA and CEB. Thus the overall convergence of CEC is much better than that of CEA and CEB. This result was rather unexpected; at the beginning of this work, our expectation was that CEA or CEB would have better convergence.

Unfortunately, the variance of the cluster contributions is the largest in CEC, presumably because in CEA and CEB each  $c_{ij\dots}$  samples all the single-particle states, whereas  $c_{ij\dots}$  in CEC samples only the single-particle states  $\phi_i\phi_j\dots$  occupied by  $ij\dots$  in  $\Phi_p$  [Eq. (3.29)].

The variance of  $T(4b)$  and  $v_6(4b)$  is so large in CEC that the sampling error in CEC  $T(4b)$  and  $v_6(4b)$ , in calculations using 10000 configurations, is much larger than the  $T(4b)$  and  $v_6(4b)$  in CEA and CEB. Thus, even though the values of  $T(4b)$  and  $v_6(4b)$  may be smaller in CEC than in CEA and CEB, it is impractical to use CEC to calculate them.

The variance of  $V(3b)$  and  $V(4b)$  is generally smaller than that of the corresponding cluster contributions to  $T$  and  $v_6$ . This could be because of the large number (560) of three-body interactions in  $^{16}\text{O}$ . Hence CEC can be used to calculate  $V$  with sampling errors  $\sim 0.1$  MeV/nucleon. Thus the optimum way to calculate  $\bar{E}_{6,v}$  with this approach seems to be to use CEA for  $T$  and  $v_6$  and CEC for  $V$ . With 10000 configurations, the statistical error in this calculation of  $\bar{E}_{6,v}$  is  $\lesssim 0.2$  MeV/nucleon.

It is necessary to include the small contributions  $T(4b)$  and  $v_6(4b)$  in the variational calculation. Optimization of variational parameters without including  $T(4b)$  and  $v_6(4b)$  leads to wave functions for which  $T(4b)+v_6(4b)$  are large and positive, so that truncation at the three-body level is not valid.

The convergence of CEA is so good for  $T$  and  $v_6$  that the expected values of  $T(nb)$  and  $v_6(nb)$  for  $n \geq 5$  are much less than 0.1 MeV/nucleon and negligible in the present context. The contributions of  $V^{2\pi}(nb)$  for  $n \geq 5$  are estimated assuming uniform convergence, i.e., by using

$$\frac{V^{2\pi}[(n+1)b]}{V^{2\pi}[nb]} = \frac{V^{2\pi}(4b)}{V^{2\pi}(3b)}. \quad (5.1)$$

In Table I the values of the sum of  $V^{2\pi}(5b)$  to  $V^{2\pi}(16b)$  obtained with Eq. (5.1) are listed along with those for  $V^R$  estimated similarly under the column titled "5-16b." It is rather comforting to note that, when the estimated contributions of  $n$ -body clusters having  $n > 4$  are added to the calculated  $n \leq 4$  contributions, the total values for  $V^{2\pi}$  and  $V^R$  listed under the column "sum" in Table I for CEA, CEB, and CEC agree to within 0.1 MeV/nucleon.

TABLE II. Statistical errors in the calculation of  $\bar{E}_{6,v}$  in MeV/nucleon for 10000 configurations.

		1b	2b	3b	4b	1-4b sum
$T$	CEA	0.13	0.13	0.17	0.20	0.30
	CEB	0.13	0.15	0.19	0.24	0.35
	CEC	0.18	0.17	0.51	0.84	0.98
$v_6$	CEA		0.24	0.15	0.26	0.30
	CEB		0.24	0.16	0.30	0.32
	CEC		0.23	0.37	0.88	0.92
$V$	CEA			0.05	0.05	0.06
	CEB			0.05	0.07	0.05
	CEC			0.04	0.10	0.11
$\bar{E}_{6,v}$	CEA	0.13	0.16	0.14	0.16	0.10
	CEB	0.13	0.16	0.15	0.19	0.12
	CEC	0.18	0.19	0.23	0.81	0.60

## VI. GROUND-STATE ENERGY AND WAVE FUNCTION

We obtain  $\bar{E}_{6,v} = -7.05 \pm 0.05$  MeV/nucleon from an average including  $\sim 40\,000$  configurations. It contains an estimate of the 5-16b cluster contributions to  $V$  as discussed in the last section. The  $\Delta E_{p>6}(2b) = -0.45$  MeV/nucleon; it includes the  $v_{p=7,14}(2b) = -0.87$  MeV/nucleon, the kinetic energy of  $u_{b,b\tau}$  correlations  $\Delta T(2b) = 0.40$  MeV/nucleon and a change  $\Delta v_6(2b) = 0.02$  MeV/nucleon due to  $u_{b,b\tau}$  correlations. The statistical errors in  $\Delta E_{p>6}(2b)$  are negligible, and this term is the same for wave functions  $\Psi_v$  and  $\bar{\Psi}_v$  because the three-body  $U_{ijk}$  correlations do not contribute to the two-body clusters.

The optimum values of the variational parameters are determined by minimizing the approximate energy  $\bar{E}_{6,v} + \Delta E_{p>6}(2b)$ , and the results given above and in Sec. V are with the optimum  $\Psi_v$ . The correction  $E_{6,v} - \bar{E}_{6,v}$  is found to be only  $-0.19 \pm 0.07$  MeV/nucleon. It includes changes of 0.27(6),  $-0.14(2)$ , and  $-0.32(2)$  in  $T(3-4b)$ ,  $v_6(3-4b)$ , and  $V(3-4b + \text{estimate for } 5-16b)$ , respectively. Thus the total variational ground-state energy of  $^{16}\text{O}$  for the Argonne  $v_{14}$  and Urbana VII interactions and the present  $\Psi_v$  is  $-7.7 \pm 0.1$  MeV/nucleon against the experimental value of  $-7.98$  MeV/nucleon.

The optimum values for the parameters of the single-particle potential [Eq. (2.18)] used to calculate the  $\Phi$  are

$$\begin{aligned} R_s &= 3.1 \text{ fm}, \quad a_s = 0.5 \text{ fm}, \\ \alpha_s &= 0.3, \quad \rho_s = 1.0 \text{ fm}, \\ V_s &= -49.1 \text{ MeV}. \end{aligned} \quad (6.1)$$

The binding energies of the 1s and 1p states are, respectively, 28.1 and 14 MeV for this potential. No statistically significant improvement of  $E_v$  could be obtained by introducing a spin-orbit splitting in the potential well.

The parameters used to determine the two-body correlations  $f_c(r)$  and  $u_p(r)$  [Eqs. (2.19)–(2.25)] are

$$\begin{aligned} d &= 2.5 \text{ fm}, \quad d_t = 4.4 \text{ fm}, \\ \beta_\sigma &= 0.95, \quad \beta_t = 1.05, \\ \alpha &= 0.94, \quad k_F = 1.1 \text{ fm}^{-1}. \end{aligned} \quad (6.2)$$

The parameters of the three-nucleon correlation  $U_{ijk}$  [Eqs. (2.29)–(2.32)] are

$$\varepsilon = -0.0015, \quad b' = 1.6 \text{ fm}^{-2}. \quad (6.3)$$

The value of the cutoff,  $b$ , is  $2 \text{ fm}^{-2}$  in the three-nucleon interaction  $V_{ijk}$ . The  $U_{ijk}$  correlation lowers the energy of  $^{16}\text{O}$  by 0.85 MeV/nucleon; it changes  $T$ ,  $v_6$ , and  $V$  by, respectively, 2.0,  $-1.4$ , and  $-1.45$  MeV/nucleon.

The parameters of  $f_3(r_{ij}; r_{ik}, r_{jk})$  [Eqs. (2.26)–(2.28)] have the values

$$t_1 = 4, \quad t_2 = 4, \quad t_3 = 0.2 \text{ fm}^{-1}. \quad (6.4)$$

The  $f_3$  factors lower the energy of  $^{16}\text{O}$  by only  $0.04 \pm 0.05$  MeV/nucleon, and thus the value of parameters  $t_{1-3}$

given above have limited significance. The variational energy of  $^4\text{He}$  [3] is lowered from  $-7.0$  MeV/nucleon by 0.4 MeV/nucleon when the  $U_{ijk}$  is included and by 0.2 MeV/nucleon when the  $f_3$  is included, to a total of  $-7.62 \pm 0.01$  MeV/nucleon. It appears that the present form of  $f_3$  [Eq. (2.27)] is more beneficial in  $^4\text{He}$  than in  $^{16}\text{O}$ .

We have made a number of attempts to improve our variational bound on the  $^{16}\text{O}$  binding energy by modifying the structure of the wave function. Two of these are described here. In the first, we broke the symmetrized product of two-body correlations into two separate symmetrized products:

$$\mathcal{S} \prod_{i<j} (1 + U_{ij}) \rightarrow \left[ \mathcal{S} \prod_{i<j} (1 + U_{ij}^t) \right] \left[ \mathcal{S} \prod_{i<j} (1 + U_{ij}^\sigma) \right], \quad (6.5)$$

$$U_{ij}^t = \sum_{p=5,6} \beta_p u_p(r_{ij}) O_{ij}^p, \quad (6.6)$$

$$U_{ij}^\sigma = \sum_{p=2,3,4,7,8} \beta_p u_p(r_{ij}) O_{ij}^p. \quad (6.7)$$

The rationale for this modification was that by having the important tensor operators act last, the other spin correlations would not interfere with them. We were able to achieve the same variational energy with this form as with Eq. (2.9), but no improvement was found.

The second modification was to introduce a backflow correlation in the one-body orbitals:

$$\phi_{lm}(\mathbf{r}_i) \rightarrow \phi_{lm}(\mathbf{r}'_i), \quad (6.8)$$

$$\mathbf{r}'_i = \mathbf{r}_i + \sum_{j \neq i} \eta(r_{ij})(\mathbf{r}_i - \mathbf{r}_j), \quad (6.9)$$

$$\eta(r) = \lambda_\eta \exp\{-[(r - r_\eta)/\omega_\eta]^2\}, \quad (6.10)$$

where  $\lambda_\eta$ ,  $r_\eta$ , and  $\omega_\eta$  are variational parameters. Such a correlation significantly improves the variational energies [19] of drops of liquid  $^3\text{He}$ . We also hoped that it would reduce the density oscillation discussed in Sec. VII, produced by the present  $\Psi_v$ . However, the best energy appears to be for  $\lambda_\eta = 0$ . Small values of  $\lambda_\eta$  that produced statistically insignificant changes in  $E_v$  do not give significant changes in the density profile.

## VII. COMPARISONS WITH FEW-BODY NUCLEI AND NUCLEAR MATTER

It is interesting and instructive to compare the results obtained with Argonne  $v_{14}$  and Urbana VII for  $^2\text{H}$ ,  $^3\text{He}$ ,  $^4\text{He}$ ,  $^{16}\text{O}$ , and nuclear matter at its equilibrium density  $\rho = 0.16 \text{ fm}^{-3}$ , as well as at the density  $\rho = 0.09 \text{ fm}^{-3}$ , corresponding to the value of  $k_F$  used in calculating the pair-correlation functions for  $^{16}\text{O}$ . The expectation values of several operators of interest are compared in Table III. They are calculated with the exact wave function for  $^2\text{H}$ , variational wave functions containing  $f_c$ ,  $U_{ij}$ ,  $U_{ijk}$ , and  $f_3$  for  $^3\text{He}$ ,  $^4\text{He}$ , and  $^{16}\text{O}$ , and with  $\Psi_v$  containing only  $f_c$  and  $U_{ij}$  for nuclear matter. The results for  $^3\text{He}$  and  $^4\text{He}$  are from complete MC integrations [3], those for  $^{16}\text{O}$  are from the present CMC, and the nuclear matter expectation values are calculated with Fermi hypernetted and operator chain summation methods [5].

The kinetic energy and the one-pion-exchange interac-

TABLE III. Expectation values in MeV/nucleon; n.m. denotes nuclear matter at the specified density.

	$^2\text{H}$	$^3\text{He}$	$^4\text{He}$	$^{16}\text{O}$	n.m. 0.09 fm $^{-3}$	n.m. 0.16 fm $^{-3}$
$T$	9.6	17.1	28.7	34.4	29	45
$v^\pi$	-11.2	-15.9	-28.2	-30.7	-27	-39
$v^\pi(N)$	-12.1	-16.7	-29.3	-31.3	-28	-41
$v^R$	0.5	-3.6	-6.1	-9.7	-10	-17
$V^{2\pi}$	0	-0.8	-3.3	-4.6	-1.8	-4.4
$V^R$	0	0.2	1.1	2.1	1.3	3.9
$v_{\text{Coul}}$	0	0.22	0.19	0.86	0	0
$E_v$	-1.11	-2.7	-7.6	-7.7	-9	-12
$E_0$	-1.11	-2.8	-7.9			
$E_{\text{expt}}$	-1.11	-2.6	-7.1	-8.0		-16

tion  $v^\pi$  give the largest contributions to the energy. The  $v^\pi$  has model-dependent short-range cutoffs. However, the model dependence of  $v^\pi$  is not very large; for example, the expectation values of  $v^\pi$  in the Argonne and Nijmegen interactions, listed in the lines  $v^\pi$  and  $v^\pi(N)$  in Table III, are quite similar. The rest of the two-nucleon interaction (excluding Coulomb),

$$v_{ij}^R \equiv v_{ij} - v_{ij}^\pi, \quad (7.1)$$

gives a contribution comparable to the total energy for  $A \geq 3$ . One could separate the  $v_{ij}^R$  into a repulsive short-range part  $v_{ij}^S$  and an attractive intermediate-range part  $v_{ij}^I$ . However, the  $v_{ij}^S$  and  $v_{ij}^I$  are much more model dependent than the  $v^\pi$ ; they give large positive and negative contributions of the order of 100 MeV. With the Argonne  $v_{14}$  interaction, the contribution of  $v^\pi$  is several times that of  $v^R$ .

The total  $E_v$  per nucleon is compared with the exact ground-state energy  $E_0$  for  $^3\text{He}$  and  $^4\text{He}$  calculated with the Faddeev [1] and GFMC [2] methods, respectively. The  $E_v$  is exact for the deuteron because the pair correlations are calculated from Euler-Lagrange equations. In principle, if the  $U_{ijk}$  and  $f_3$  are correctly chosen, the  $E_v$  should also be exact for  $^3\text{He}$ . The 0.1-MeV difference between  $E_0$  and  $E_v$  of  $^3\text{He}$  indicates that these functions are not yet fully optimized. Attempts to extract the  $U_{ijk}$  and  $f_3$  from the Faddeev wave function are in progress; these could reduce the error in  $E_v$  substantially. The error in the total (not per nucleon) variational energy of  $^4\text{He}$  is 1.1 MeV, while that in  $^3\text{He}$  is 0.28 MeV. There are four triplets in  $^4\text{He}$ , and so it is possible that variational calculations with the proper  $U_{ijk}$  and  $f_3$  would be very accurate for  $^4\text{He}$ .

The error in the  $E_v$  of  $^{16}\text{O}$  is very difficult to estimate

reliably; it is certainly larger than that in the present  $E_v$  of  $^4\text{He}$ . If the error in  $E_v$  is entirely due to inaccurate representation of the three-body correlations in  $\Psi_v$ , it will approximately scale with  $V^{2\pi}$  and become  $\sim 0.5$  MeV/nucleon in  $^{16}\text{O}$ .

The  $E_v$  of nuclear matter calculated with the Urbana rather than Argonne  $v_{ij}$  has been lowered by 1.7 MeV at  $\rho = 0.16 \text{ fm}^{-3}$  by adding two-particle, two-hole corrections to  $\Psi_v$  perturbatively [24]. A correction of this magnitude can also be inferred from the comparison of results obtained with the variational and Brueckner-Bethe calculations [4] with Argonne  $v_{ij}$ . The  $E_v$  of nuclear matter with  $v_{ij}$  and  $V_{ijk}$  might be lowered further by  $\sim 1$  MeV by including the  $U_{ijk}$  in the  $\Psi_v$ . A detailed comparison of the contributions of the various  $v_p$ 's to the energy, shown in Table IV, suggests that the calculated expectation values of  $v_{p=9,14}$  may be too large in nuclear matter. In the few-body nuclei and  $^{16}\text{O}$ , these interactions contribute mostly through the  $^3D_1$  state in which their sum is small and negative. In  $^2\text{H}$ ,  $^3\text{He}$ , and  $^4\text{He}$ , the L·S interactions also contribute mostly via the  $^3D_1$  state in which their sum is repulsive. In  $^{16}\text{O}$  and nuclear matter, the L·S interactions give a small negative contribution via the  $P$  waves and L·S correlations. Without the L·S correlations, the  $P$  waves give a negligible contribution, and  $v_{p=7,8}$  becomes  $+0.55$  MeV/nucleon in  $^{16}\text{O}$ , again dominated by the  $^3D_1$  state.

The experimental energies of  $^2\text{H}$ ,  $^3\text{He}$ ,  $^4\text{He}$ , and  $^{16}\text{O}$ , and the empirical nuclear matter energy are also listed in Table III. The Urbana VII model of  $V_{ijk}$  is not very realistic; the exact  $E_0$  obtained with it for  $^3\text{He}$  and  $^4\text{He}$  is too low. The Urbana VIII model [3] of  $V_{ijk}$  has a weaker  $V_{ijk}^{2\pi}$  and a stronger  $V_{ijk}^R$  adjusted to give the observed energies of  $^3\text{H}$  and  $^4\text{He}$  in exact calculations. However, the

TABLE IV. Expectation values of the  $v_p$ 's in MeV/nucleon; n.m. denotes nuclear matter at the specified density.

	$^2\text{H}$	$^3\text{He}$	$^4\text{He}$	$^{16}\text{O}$	n.m. 0.09 fm $^{-3}$	n.m. 0.16 fm $^{-3}$
$v_{p=1,6}$	-10.4	-19.2	-34.3	-39.6	-37	-57
$v_{p=7,8}$	0.18	0.24	0.50	-0.36	-0.6	-1.5
$v_{p=9,14}$	-0.49	-0.49	-0.46	-0.41	0.8	2.7

$E_v$  obtained with it for  $^{16}\text{O}$  is only  $-6.4$  MeV/nucleon. Even if we assume that the present  $E_v$  of  $^{16}\text{O}$  is as much as  $0.5$  MeV/nucleon above the true  $E_0$ ,  $^{16}\text{O}$  is underbound with the Urbana VIII model.

### VIII. DENSITY AND MOMENTUM DISTRIBUTIONS AND RELATED OBSERVABLES

The results obtained with CEA for the point nucleon density distribution  $\rho(r)$  of  $^{16}\text{O}$  are shown in Fig. 1, along with the  $\rho(r)$  obtained from the independent-particle wave function  $\Phi$ . The two-body ( $2b$ ) cluster contributions to the  $\rho(r)$  are significant, while those of the four-body ( $4b$ ) clusters are negligible except at small  $r$ . The solid curve in Fig. 1 shows the sum of the Jastrow and  $2b$  contributions without any estimate made for  $3b$  contributions.

The “experimental”  $\rho(r)$  shown in Fig. 1 is obtained by unfolding a dipole proton form factor from the published [25] charge distributions and by assuming that the neutrons and protons have identical density distributions. The exchange-current as well as neutron contributions are neglected in this extraction of the “experimental” density from the observed data. The calculated  $\rho(r)$  has a much larger oscillation than the data; the oscillation comes primarily from  $\phi$  and is enhanced by the noncentral correlations. In contrast, in drops of atomic liquid  $^3\text{He}$ , the pair correlations substantially smooth out the density profile generated by the  $\Phi$  [19]. The rms point nucleon radius given by  $\Phi$ ,  $\Psi_v$ , and “experiment” are  $2.60$ ,  $2.43$ , and  $2.62$  fm, respectively.

The charge form factor  $F_c(k)$  of  $^{16}\text{O}$  is calculated using the one- and two-body charge operators given by Schiavilla, Pandharipande, and Riska [26]. The results, including up to four-body cluster contributions, are compared with the experimental data [27] in Fig. 2. The contributions of  $\pi$ -,  $\rho$ -, and  $\omega$ -exchange two-body charge operators reduce the difference between theory and experiment for  $k > 2$  fm $^{-1}$ ; however, they are negligible at

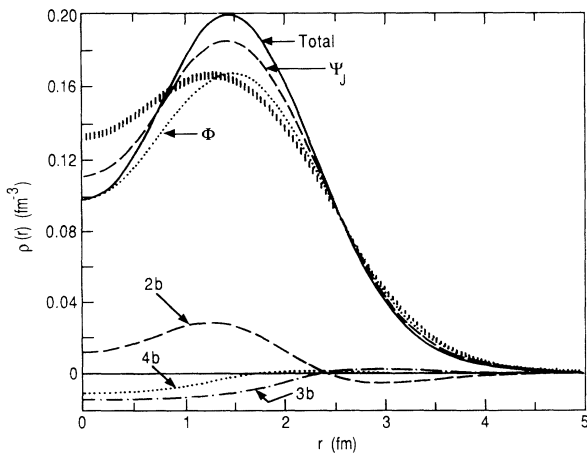


FIG. 1. Density distributions obtained from the  $\Psi_v$ ,  $\Psi_J$ , and  $\Phi$  compared with the “experimental” data, shown by the shaded region. The contributions of  $2b$  clusters to the  $\rho(r)$  from  $\Psi_v$  are also shown.

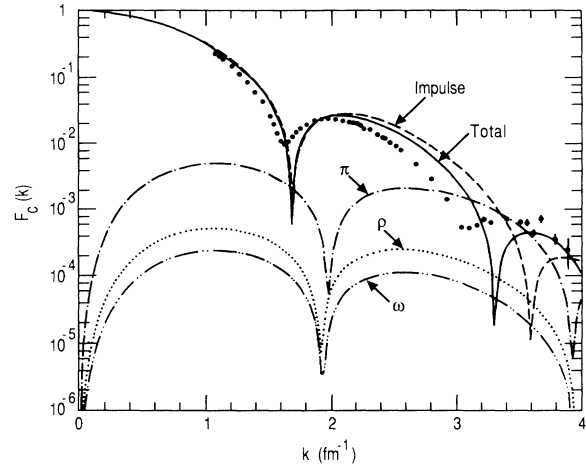


FIG. 2. Charge form factor obtained from the  $\Psi_v$  compared with the experimental data [27]. The form factor obtained in the impulse approximation and the contributions of the  $\pi$ -,  $\rho$ -, and  $\omega$ -exchange terms are also shown.

$k < 2$  fm $^{-1}$ . The Iachello-Jackson-Lande [28] nucleon form factors are used in these calculations, but at the small values of  $k$  ( $< 4$  fm $^{-1}$ ) of interest here, the differences between the various models of the nucleon form factor discussed in Ref. [26] are small.

The failure of our calculation to reproduce the observed  $F_c(k)$  is directly related to the excessive oscillation of the calculated  $\rho(r)$ . Charge form factors in good agreement with the data can be obtained by changing the  $\Phi$ , i.e., parameters given in Eq. (6.1). However, the energy is raised by  $\sim 0.5$  MeV/nucleon in this process so that  $\Phi$ 's that explain the observed  $F_c(k)$  are variationally excluded. Moreover, if we change  $\Phi$  to obtain better  $F_c(k)$  and then reoptimize the pair correlations by minimizing the energy, most of the improvement in  $F_c(k)$  obtained by changing the  $\Phi$  is lost. These results suggest that the failure to reproduce the experimental  $F_c(k)$  is due to the present Hamiltonian and not due to inadequacies in the variational calculation. However, this Hamiltonian gives a fairly good description of the observed form factors of hydrogen and helium isotopes [29].

The momentum distribution  $n(k)$  of nucleons in  $^{16}\text{O}$  is calculated using CEB and a method described elsewhere [30]; the results are shown in Fig. 3. The  $n(k)$  given by  $\Phi$  is obtained from the Fourier transforms of the single-particle orbitals  $\phi_{nlm}(\mathbf{r})$ . It is shown by the dotted line, while the  $n(k)$  for the Jastrow wave function is shown by the dot-dashed curve. The dashed curve shows the  $n(k)$  obtained on including the contributions of two-body clusters. These two-body contributions, which come primarily from the tensor correlations, are much larger than those of  $\Psi_J$  in the  $2$ – $3.5$ -fm $^{-1}$  region and remain 4 times bigger for larger momenta.

The three-body clusters give a small contribution to  $n(k)$ ; the calculated total  $n(k)$  including three-body contributions is shown by the solid curve in Fig. 3. We expect the four-body cluster contributions to  $n(k)$  to be smaller than the statistical error obtainable with a

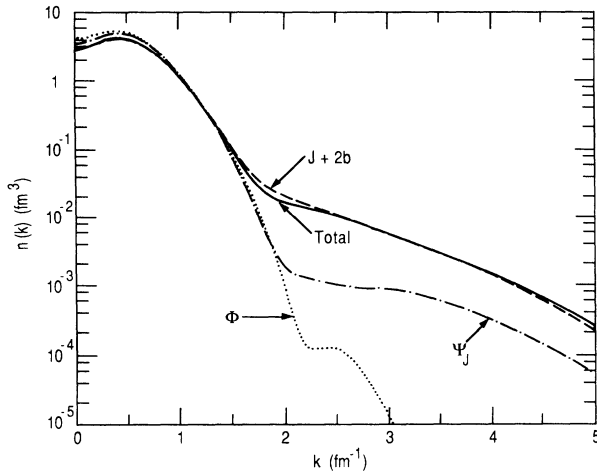


FIG. 3. Cumulative cluster contributions to  $n(k)$ .

reasonable amount of computer time. The statistical errors of the curves in Figs. 3 and 4 are negligible.

The  $n(k)/A$  obtained with the present Hamiltonian for  $^2\text{H}$ ,  $^4\text{He}$ , [3],  $^{16}\text{O}$ , and with the Urbana  $v_{ij}$  without  $V_{ijk}^{2\pi}$  for nuclear matter [31], are compared in Fig. 4. Note that for  $k > 2 \text{ fm}^{-1}$  the  $^4\text{He}$ ,  $^{16}\text{O}$ , and nuclear matter  $n(k)/A$  are in very close agreement with each other. Since the Argonne  $v_{14}$  has a stronger tensor force and since the  $V_{ijk}^{2\pi}$  enhances the tensor correlations, it is likely that the nuclear matter  $n(k > 2 \text{ fm}^{-1})/A$  obtained with the present Hamiltonian will be larger than that from Ref. [31] shown in Fig. 4. In particular, the noncentral correlations give only half of the  $n(k)$  at large  $k$  in nuclear matter with Urbana  $v_{ij}$ , whereas they give approximately three-quarters of the total in the present calculation.

The two-particle density distribution  $\rho_{12}(r)$  is defined as

$$\rho_{12}(r) = \frac{1}{4\pi r^2 A} \sum_{i \neq j} \langle \Psi_v | \delta(r - |\mathbf{r}_i - \mathbf{r}_j|) | \Psi_v \rangle \quad (8.1)$$

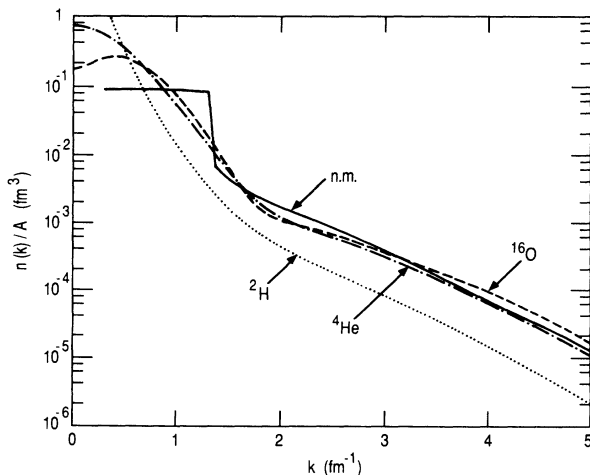


FIG. 4.  $n(k)/A$  in  $^2\text{H}$ ,  $^4\text{He}$ ,  $^{16}\text{O}$ , and nuclear matter.

and has the normalization

$$4\pi \int dr r^2 \rho_{12}(r) = A - 1. \quad (8.2)$$

It is proportional to the probability of finding a pair of nucleons separated by a distance  $r$  in the nucleus. The cluster contributions to  $\rho_{12}(r)$  and the total  $\rho_{12}(r)$  obtained with CEA are shown in Fig. 5. The expansion seems to converge very well for the  $\rho_{12}(r)$ , and the statistical errors are negligible in the results shown here.

The two particle densities  $\rho_{pp}(r)$  and  $\rho_{pn}(r)$  are defined as

$$\rho_{pN}(r) = \frac{1}{4\pi r^2 Z} \sum_{i \neq j} \langle \Psi_v | \delta(r - |\mathbf{r}_i - \mathbf{r}_j|) P_p(i) P_N(j) | \Psi_v \rangle, \quad (8.3)$$

where  $P_N(i)$  are the projection operators  $[1 \pm \tau_3(i)]/2$  for  $p$  and  $n$ . The  $\rho_{pp}(r)$  and  $\rho_{pn}(r)$ , respectively, give the distribution of protons and neutrons around a proton, and in systems such as  $^{16}\text{O}$ , having total isospin  $T=0$ ,

$$\rho_{12} = \rho_{pp} + \rho_{pn}. \quad (8.4)$$

The distribution of particles around a neutron is given by  $\rho_{nn}$  and  $\rho_{np}$ , and in  $T=0$  systems,  $\rho_{nn} = \rho_{pp}$  and  $\rho_{np} = \rho_{pn}$ . In MC calculations of such systems, one can average over  $\rho_{nn}$  and  $\rho_{pp}$  to reduce sampling errors. The calculated  $\rho_{pn}$  and  $\rho_{pp}$  are shown in Fig. 6. At large  $r$ ,  $\rho_{pn} \sim \rho_{pp}$ , but at small  $r$ ,  $\rho_{pp} < \rho_{pn}$  as a result of Pauli exclusion. Note that Eq. (8.3) implies that

$$\int 4\pi r^2 dr [\rho_{pn}(r) - \rho_{pp}(r)] = 1, \quad (8.5)$$

in the  $T=0$  systems.

The  $\rho_{NN}(r=0)$  are very small because of the correlations induced by the repulsive core in the two-nucleon interaction. The  $\rho_{NN}(r)$  calculated from an independent-particle wave function  $\Phi_{\text{MF}}$ , which has the same  $\rho(r)$  as the  $\Psi_v$ , are also shown in Fig. 6 by curves labeled MF for mean field. The  $\Phi_{\text{MF}}$  are calculated using the methods described in Ref. [32]. The mean-field  $\rho_{NN}(r)$  are much too large at small  $r$ ; at large  $r$ , they provide an excellent

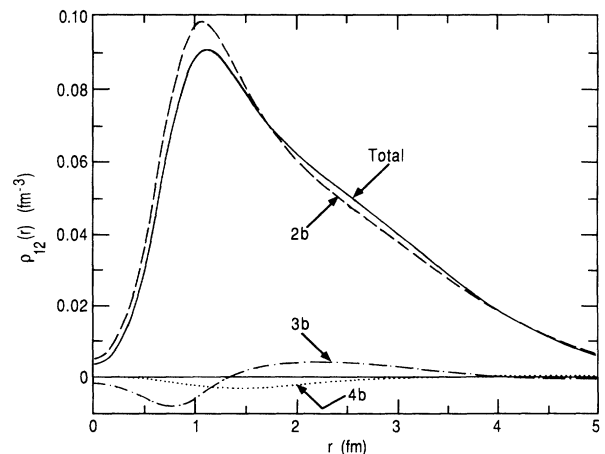


FIG. 5. Two-body density  $\rho_{12}(r)$  including contributions of 2-4b clusters.

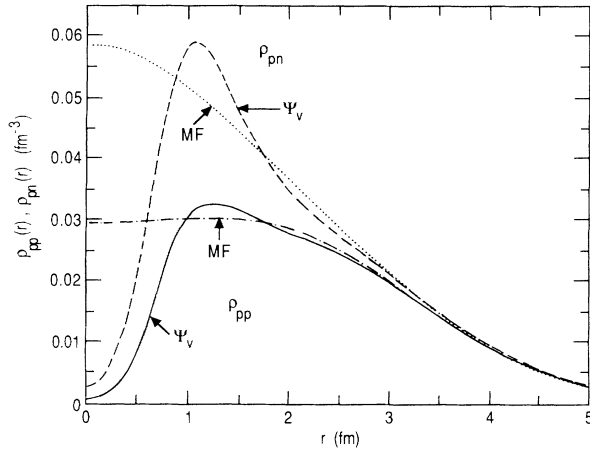


FIG. 6.  $\rho_{pp}(r)$  and  $\rho_{pn}(r)$  calculated from  $\Psi_v$  and  $\Phi_{MF}$ .

approximation to the complete calculation.

In finite systems, the  $\rho_{12}(r \rightarrow \infty) \rightarrow 0$ , whereas, in infinite nuclear matter at density  $\rho$ , the  $\rho_{12}(r \rightarrow \infty) \rightarrow \rho$ . Since the maximum value of  $\rho_{12}$  in  $^{16}\text{O}$  is only  $0.09 \text{ fm}^{-3}$ , it is not surprising that the optimal pair correlations in  $^{16}\text{O}$  correspond to those in nuclear matter at  $\rho \sim 0.09 \text{ fm}^{-3}$ , as found in the variational search.

The Coulomb sum, or equivalently the longitudinal structure function  $S_L(k)$ , is the integral over  $\omega$  of the longitudinal response function  $S_L(k, \omega)$  measured in electron-nucleus scattering experiments. It is primarily determined by the Fourier transform of  $\rho_{pp}(r)$ :

$$S_L(k) = \tilde{\rho}_{pp}(k) + 1 - \frac{1}{Z} |\tilde{\rho}_p(k)|^2 + \text{corrections}, \quad (8.6)$$

where  $\tilde{\rho}_p(k)$  is the Fourier transform of the proton density distribution  $\rho_p(r)$ . At small  $k$  the main correction is from the contribution of neutrons to the longitudinal scattering, as discussed in Ref. [32]. The contributions of  $2b$ - $4b$  clusters to  $S_L(k)$  are shown in Fig. 7. It is necessary to include the  $3b$  cluster contributions to ensure that  $S_L(k) \geq 0$  as it must be for any system.

The  $S_L(k=0) = 0$  for any system. This fundamental property of  $S_L(k)$  is preserved in each order of CEA, which conserves the number of  $nn$ ,  $pp$ , and  $np$  pairs in each order. In contrast, the  $S_L(k=0)$  calculated with CEB or CEC is not necessarily zero when the expansions are truncated. For this reason CEA has been used in all the studies of the two-body density functions.

The  $S_L(k)$  of  $^4\text{He}$  and nuclear matter [32] are compared with the present results for  $^{16}\text{O}$  in Fig. 8. The dashed line in Fig. 8 is obtained from the mean-field wave function  $\Phi_{MF}$ . The relatively small difference between the  $S_L(k)$  obtained with the  $\Phi_{MF}$  and  $\Psi_v$  is due to the correlations. There are no data on the  $S_L(k)$  of  $^{16}\text{O}$ ; the data shown in Fig. 8 are for  $^{12}\text{C}$  from Ref. [33] with an estimate [34] for contributions from large  $\omega$ .

We define two-body densities  $\rho_{2,p}(r)$  associated with the operators  $O_{ij}^p$  as

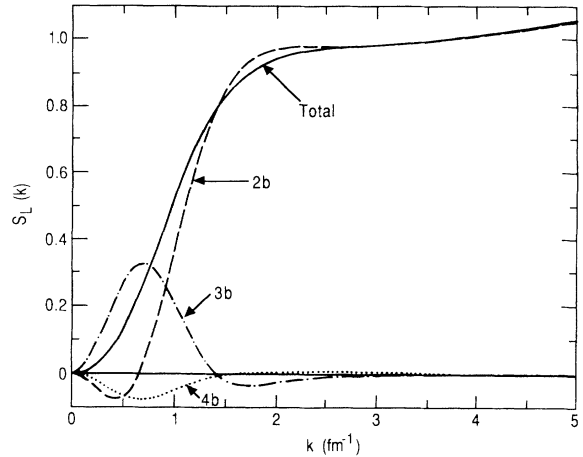


FIG. 7. Longitudinal structure function  $S_L(k)$ , including contributions of  $2$ - $4b$  clusters.

$$\rho_{2,p}(r) = \frac{1}{4\pi r^2 A} \sum_{i < j} \frac{\langle \Psi_v | \delta(r - |\mathbf{r}_i - \mathbf{r}_j|) O_{ij}^p | \Psi_v \rangle}{\langle \Psi_v | \Psi_v \rangle}. \quad (8.7)$$

These densities are very useful and are shown in Fig. 9. For example, the expectation value of an operator  $B$ ,

$$B = \sum_p \sum_{i < j} B_p(r_{ij}) O_{ij}^p, \quad (8.8)$$

is given by

$$\langle B \rangle = 2\pi A \sum_p \int r^2 dr B_p(r) \rho_{2,p}(r). \quad (8.9)$$

The  $\sigma\tau$  and  $t\tau$  operators have large two-body densities which give the large  $\langle v^\pi \rangle$  shown in Table III.

## IX. CONCLUSIONS

The proposed CMC method appears to provide a way by which accurate variational calculations can be carried

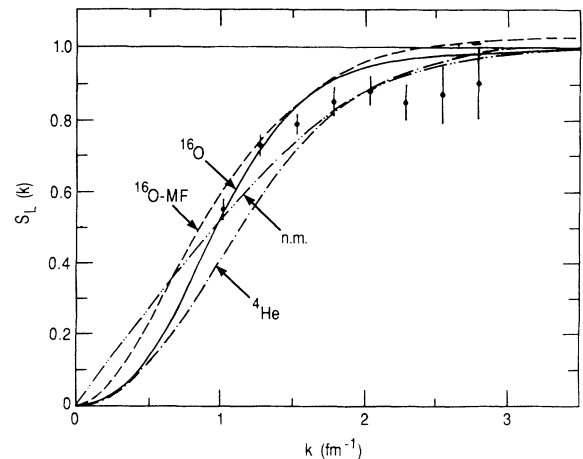


FIG. 8.  $S_L(k)$  obtained with  $\Psi_v$  and  $\Phi_{MF}$  compared with the  $S_L(k)$  of  $^4\text{He}$  and nuclear matter calculated from their  $\Psi_v$ . The data points show the "experimental"  $S_L(k)$  of  $^{12}\text{C}$  from Refs. [33,34].

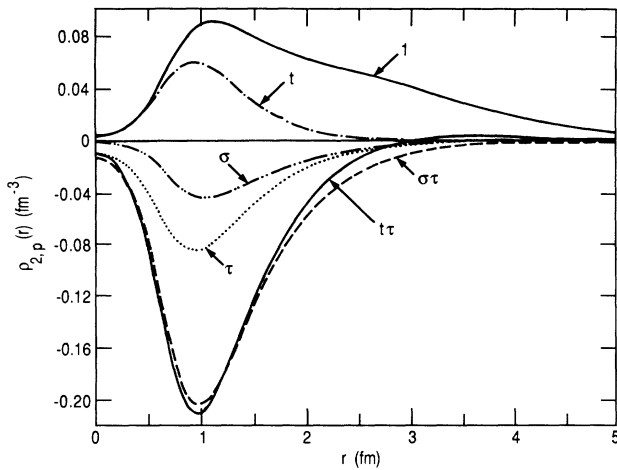


FIG. 9. Two-body densities  $\rho_{2,p}(r)$  in  $^{16}\text{O}$ .

out with realistic nuclear forces. The simpler VMC method is limited to nuclei having  $A \leq 8$ , and hence the CMC is, at present, the only variational method useful for larger nuclei. It appears to be necessary to include four-body clusters in the calculation, which increases the required computational effort substantially. Nevertheless, calculations of the properties of  $^{15}\text{N}$ ,  $^{16}\text{O}$ , and  $^{17}\text{O}$  are possible with available computers.

It should be possible to extend the CMC to lighter nuclei such as  $^8\text{He}$  and  $^{12}\text{C}$  and heavier nuclei such as  $^{40}\text{Ca}$ . However, these extensions are not completely trivial. In  $^8\text{He}$  and  $^{12}\text{C}$ , the  $\Phi$  cannot be well approximated by an antisymmetric product of four determinants, though it is possible to express it as a sum of such products. In heavier nuclei the number of four-body clusters increases approximately like  $A^4$ ; it is 91 390 in  $^{40}\text{Ca}$  compared with 1720 in  $^{16}\text{O}$ . However, it is possible to sample only a fraction of the four-body clusters in CMC. In an unoptimized test CMC calculation of  $^{40}\text{Ca}$  with the present Hamiltonian, we sampled only 1720 four-body clusters per configuration and obtained  $E_v = -8.9 \pm 1.5$  MeV/nucleon in 8 h of Cray-2 computer time.

The statistical error in the present calculation of  $E_v$  for  $^{16}\text{O}$ , estimated to be 0.1 MeV/nucleon, is tolerable. Unfortunately the difference between the present  $E_v$  and the true  $E_0$  is much larger, probably  $\gtrsim 0.5$  MeV/nucleon in

$^{16}\text{O}$  as discussed in Sec. VII, and more difficult to estimate. In few-body nuclei, it is possible to improve upon the VMC by a GFMC calculation [2] and obtain the true  $E_0$ . At present, it is not known if a similar development of CMC is possible.

One of our objectives is to constrain the form and determine the parameters of the three-nucleon interaction  $V_{ijk}$  by fitting the observed properties of nuclei. This  $V_{ijk}$  can then be used to predict the equation of state of nuclear matter, the structure of neutron stars [5], and to probe nuclear structure in greater detail. The results of the present calculations suggest that the Urbana VII  $V_{ijk}$  has two problems in addition to the overbinding of  $^3\text{H}$  and  $^4\text{He}$  it predicts. First, the difference between the  $E_v$ 's of  $^4\text{He}$  and  $^{16}\text{O}$  is only  $0.1 \pm 0.1$  MeV/nucleon, whereas the experimental value is 0.9 MeV/nucleon. The difference between the true  $E_0$ 's with this  $V_{ijk}$  is not known, but it is likely to be less than 0.9 MeV/nucleon. The present calculations suggest that this  $V_{ijk}$  does not contribute significantly to this difference. Variational calculations with the Argonne  $v_{ij}$ , without any  $V_{ijk}$ , also give a  $0.1 \pm 0.1$ -MeV/nucleon difference in the  $E_v$ 's of  $^4\text{He}$  and  $^{16}\text{O}$ ; the  $E_v$ 's without  $V_{ijk}$  are, respectively,  $-5.88(1)$  [3] and  $-6.0(1)$  for  $^4\text{He}$  and  $^{16}\text{O}$ . Second, the oscillation in the  $\rho(r)$  of  $^{16}\text{O}$  predicted by the Argonne  $v_{ij}$  and Urbana VII  $V_{ijk}$  is approximately 3 times larger than inferred from experiment.

Finally, the results presented here suggest at least two improvements in the variational theory of nuclear matter. The  $U_{ijk}$  correlations induced by the  $V_{ijk}$  should be included, and the contribution of the  $p=9-14$  terms in the latest [5] calculations of  $E(\rho)$  for nuclear matter is suspiciously large.

#### ACKNOWLEDGMENTS

This work was supported by the U.S. Department of Energy, Nuclear Physics Division, under Contract No. W-31-109-ENG-38, and by the National Science Foundation, Grant No. PHY 89-21025. The calculations reported here were made possible by grants of time on the Cray computers at the National Energy Research Supercomputer Center, Livermore, California, and the National Center for Supercomputing Applications, Urbana, Illinois.

- [1] C. R. Chen, G.L. Payne, J. L. Friar, and B. F. Gibson, Phys. Rev. C **33**, 1740 (1986).  
 [2] J. Carlson, Phys. Rev. C **38**, 1879 (1988).  
 [3] R. B. Wiringa, Phys. Rev. C **43**, 1585 (1991).  
 [4] B. D. Day and R. B. Wiringa, Phys. Rev. C **32**, 1057 (1985).  
 [5] R. B. Wiringa, V. Fiks, and A. Fabrocini, Phys. Rev. C **38**, 1010 (1988).  
 [6] H. Kümmel, K. H. Lüthmann, and J. G. Zabolitzky, Phys. Rep. **36C**, 1 (1979).  
 [7] R. V. Reid, Ann. Phys. (N.Y.) **50**, 411 (1968).  
 [8] S. A. Coon, M. D. Scadron, P. C. McNamee, B. R. Barrett, D. W. E. Blatt, and B. H. J. McKellar, Nucl. Phys.

- A**317**, 242 (1979).  
 [9] J. Carlson, V. R. Pandharipande, and R. B. Wiringa, Nucl. Phys. A**401**, 59 (1983).  
 [10] J. Carlson and M. H. Kalos, Phys. Rev. C **32**, 2105 (1985).  
 [11] S. C. Pieper, R. B. Wiringa, and V. R. Pandharipande, Phys. Rev. Lett. **64**, 364 (1990).  
 [12] R. B. Wiringa, R. A. Smith, and T. L. Ainsworth, Phys. Rev. C **29**, 1207 (1984).  
 [13] R. Schiavilla, V. R. Pandharipande, and R. B. Wiringa, Nucl. Phys. A**449**, 219 (1986).  
 [14] M. Lacombe, B. Loiseau, J. M. Richard, R. Vinh Mau, J. Côté, P. Pirés, and R. de Tourreil, Phys. Rev. C **21**, 861 (1980).

- [15] M. M. Nagels, T. A. Rijken, and J. J. de Swart, *Phys. Rev. D* **17**, 768 (1978).
- [16] I. E. Lagaris and V. R. Pandharipande, *Nucl. Phys.* **A359**, 349 (1981).
- [17] J. Lomnitz-Adler, V. R. Pandharipande, and R. A. Smith, *Nucl. Phys.* **A361**, 399 (1981).
- [18] J. C. Owen, *Phys. Lett.* **77B**, 9 (1978).
- [19] V. R. Pandharipande, S. C. Pieper, and R. B. Wiringa, *Phys. Rev. B* **34**, 4571 (1986).
- [20] V. R. Pandharipande and R. B. Wiringa, *Rev. Mod. Phys.* **51**, 821 (1979).
- [21] D. S. Lewart and V. R. Pandharipande, in *Monte Carlo Methods in Theoretical Physics*, edited by S. Caracciolo and A. Fabrocini (ETS Editrice, Pisa, 1991).
- [22] J. Carlson and R. B. Wiringa, in *Computational Nuclear Physics I*, edited by K. Langanke, J. A. Maruhn and S. E. Koonin (Springer-Verlag, Berlin, 1991).
- [23] J. Carlson and V. R. Pandharipande, *Nucl. Phys.* **A371**, 301 (1981).
- [24] S. Fantoni, B. L. Friman, and V. R. Pandharipande, *Nucl. Phys.* **A399**, 51 (1983).
- [25] H. de Vries, C. W. de Jager, and C. de Vries, *At. Data Nucl. Data Tables* **36**, 495 (1987).
- [26] R. Schiavilla, V. R. Pandharipande, and D. O. Riska, *Phys. Rev. C* **41**, 309 (1990).
- [27] I. Sick and J. S. McCarthy, *Nucl. Phys.* **A150**, 631 (1970).
- [28] F. Iachello, A. D. Jackson, and A. Lande, *Phys. Lett.* **43B**, 191 (1973).
- [29] J. Carlson, V. R. Pandharipande, and R. Schiavilla, in *Modern Topics in Electron Scattering*, edited by B. Frois and I. Sick (World Scientific, Singapore, 1991).
- [30] J. Carlson, V. R. Pandharipande, S. C. Pieper, R. Schiavilla, and R. B. Wiringa (unpublished).
- [31] S. Fantoni and V. R. Pandharipande, *Nucl. Phys.* **A427**, 473 (1984).
- [32] R. Schiavilla, D. S. Lewart, V. R. Pandharipande, S. C. Pieper, R. B. Wiringa, and S. Fantoni, *Nucl. Phys.* **A473**, 267 (1987).
- [33] P. Barreau *et al.*, *Nucl. Phys.* **A402**, 515 (1983).
- [34] R. Schiavilla, A. Fabrocini, and V. R. Pandharipande, *Nucl. Phys.* **A473**, 290 (1987).